

Non-Fermi liquid behavior in the magnetotransport of CeMIn_5 (M : Co and Rh): Striking similarity between quasi two-dimensional heavy fermion and high- T_c cuprates

Y. NAKAJIMA^{1,2}, H. SHISHIDO¹, H. NAKAI¹, T. SHIBAUCHI¹, K. BEHNIA³, K. IZAWA^{2,4}, M. HEDO², Y. UWATOKO², T. MATSUMOTO⁵, R. SETTAI⁶, Y. ONUKI⁶, H. KONTANI⁷, and Y. MATSUDA^{1,2}

¹*Department of Physics, Kyoto University, Kyoto 606-8502, Japan*

²*Institute for Solid State Physics, University of Tokyo, Kashiwanoha, Kashiwa, Chiba 277-8581, Japan*

³*Laboratoire de physique quantique (CNRS), ESPCI, 10 Rue Vauquelin, 75005 Paris, France*

⁴*CEA-Grenoble, 38054 Grenoble Cedex 9, France*

⁵*National Institute of Material Science, Sakura, Tsukuba, Ibaraki 305-0003, Japan*

⁶*Graduate School of Science, Osaka University, Toyonaka, Osaka 560-0043, Japan*

⁷*Department of Physics, Nagoya University, Furo-cho, Chikusa-ku, Nagoya 464-8602, Japan*

We present a systematic study of the dc-resistivity, Hall effect, and magnetoresistance in the normal state of quasi two-dimensional (2D) heavy fermion superconductors CeMIn_5 (M : Rh and Co) under pressure. Here the electronic system evolves with pressure from an anti-ferromagnetic (AF) metal, through a highly unconventional non-Fermi liquid, and finally into a Fermi-liquid state. The novelty of these materials is best highlighted when compared with LaMIn_5 , a system with similar electronic structures, which shows a nearly temperature independent Hall coefficient and a magnetoresistance which is well described by the classical Kohler rule. In sharp contrast, in CeMIn_5 , the amplitude of the Hall coefficient increases dramatically with decreasing temperature, reaching at low temperatures a value significantly larger than $1/ne$, where n is the carrier number. Furthermore, the magnetoresistance is characterized by T - and H -dependence which clearly violate Kohler's rule. We found that the cotangent of the Hall angle $\cot \Theta_H$ varies as T^2 , and the magnetoresistance is well scaled by the Hall angle as $\Delta\rho_{xx}/\rho_{xx} \propto \tan^2 \Theta_H$. These non-Fermi liquid properties in the electron transport are remarkably pronounced when the AF fluctuations are enhanced in the vicinity of the quantum critical point. We lay particular emphasis on the striking resemblance of these anomalous magnetotransport with those of the high- T_c cuprates. We argue that features commonly observed in quasi 2D heavy fermion and cuprates very likely capture universal features of strongly correlated electron systems in the presence of strong AF fluctuations, holding the promise of bridging our understanding of heavy fermion systems and high- T_c cuprates.

KEYWORDS: Hall effect, magnetoresistance, Fermi liquid, heavy fermion, quantum critical point

1. Introduction

One of the most interesting and puzzling issues in the research of strongly correlated electron systems is anomalous electron transport phenomena. The dc-resistivity, Hall coefficient, and magnetoresistance are fundamental transport property parameters and it is well established that in conventional metals these transport parameters are well described by Landau's Fermi liquid theory. In the Fermi liquid state, the dc resistivity, Hall coefficient, and magnetoresistance exhibit characteristic T - and H -dependence. The dc resistivity ρ_{xx} due to electron-electron scattering depends on T as

$$\rho_{xx} \propto T^2. \quad (1)$$

The Hall coefficient R_H signifies the Fermi surface topology and carrier density; in the simple case it is given as

$$R_H = \frac{1}{ne}, \quad (2)$$

where n is the carrier number, and is independent of temperature.¹ The magnetoresistance stems from bending of the electron trajectory by the Lorentz force. The magnetoresistance can be used to probe deviations of the Fermi surface from sphericity, providing unique information on how the electron mean free path varies around the

Fermi surface. The magnetoresistance $\Delta\rho_{xx}/\rho_{xx}$ obeys Kohler's rule,

$$\frac{\Delta\rho_{xx}}{\rho_{xx}} = F\left(\frac{H}{\rho_{xx}}\right), \quad (3)$$

where $\Delta\rho_{xx} \equiv \rho_{xx}(H) - \rho_{xx}(0)$ and $F(x)$ is a function depending on the details of the electronic structure.²

Within the last decade, however, it has been found that in strongly correlated materials, including heavy fermion intermetallics, organics, and high- T_c cuprates, these transport parameters display striking deviations from Fermi liquid behavior, especially in the presence of the strong magnetic fluctuations.³⁻⁵ In each of these materials, chemical doping, pressure, or magnetic field can tune the quantum and thermal fluctuations at zero and finite temperatures. It is generally believed that the strong magnetic fluctuations seriously modify the quasi-particle masses and scattering cross section of a Fermi liquid. As a result, these systems develop a new excitation structure and often display peculiar electron transport properties over a wide temperature range. In addition, some of these metals display superconductivity. It is also generally believed that the strong electron correlation leads to a notable many-body effect and often gives rise to unconventional superconducting pair states

with angular momentum greater than zero.^{6–8} Therefore the properties of the normal state, which is the stage of the novel superconductivity, are intimately related to the mechanism of the superconducting pairing interaction.

Among strongly correlated materials, the electron transport properties of high- T_c cuprates have been studied the most extensively. In the optimally and underdoped regimes, they exhibit all the hallmarks of non-Fermi liquid behavior. In the optimally doped regime, the resistivity shows a T -linear dependence over a wide temperature range from T_c up to very high temperatures:

$$\rho_{xx} \propto T. \quad (4)$$

The Hall coefficient R_H exhibits strong, sometimes peaked, temperature and doping dependence.^{9–11} At very high temperatures, R_H is close to $1/ne$, as expected for conventional metals. However, R_H increases with decreasing temperature and attains a value much larger than $1/ne$ at low temperatures. It has been pointed out that the Hall problem can be simplified when analyzed in terms of $\cot \Theta_H$, where $\Theta_H \equiv \tan^{-1}(\rho_{xy}/\rho_{xx})$ is the Hall angle and ρ_{xy} is the Hall resistivity.^{12,13} In high- T_c cuprates, the Hall angle approximately varies as

$$\cot \Theta_H \equiv \frac{\rho_{xx}}{\rho_{xy}} \propto T^2. \quad (5)$$

The magnetoresistance does not show the scaling relation given in Eq. (3), indicating a strong violation of Kohler's rule. A new scaling relation,

$$\frac{\Delta\rho_{xx}}{\rho_{xx}} \propto \tan^2 \Theta_H, \quad (6)$$

has been proposed to describe the T - and H -dependence of the magnetoresistance.¹⁴ In the underdoped regime, ρ_{xx} and R_H are reduced below the (smaller) pseudogap temperature. In addition to these electron transport properties, the thermoelectric effects have been reported to be quite anomalous in the underdoped and optimally doped regimes. In particular a giant enhancement of the Nernst coefficient ν_H , three orders of magnitude larger than that expected for conventional metals, has been reported for high- T_c cuprates.¹⁵

Extensive experimental and theoretical studies have been made to establish a picture of the basic transport properties in non-Fermi liquid states. Two types of theoretical models have been proposed: models based on a Fermi liquid ground state, in which the carriers are electrons and holes, and more exotic models based on a non-Fermi liquid ground state, in which the transport carriers are exotic objects, such as spinons and holons. In the Fermi liquid approach, an anisotropic scattering mechanism of carriers is invoked.^{16–20} The central concept behind this is the "hot spot", a small region on the Fermi surface where the electron lifetime is unusually short, e.g., due to the electron–antiferromagnetic(AF) spin fluctuation scattering. In the non-Fermi liquid approach, the charge transport is assumed to be governed by two separate scattering times with different temperature dependence associated with spin–charge separation.^{12,13}

There appears to be common agreement on the inadequacy of the Bloch–Boltzmann approach (i.e., the

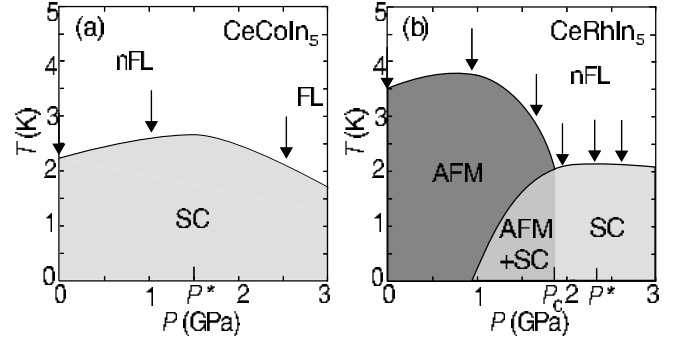


Fig. 1. Schematic P - T phase diagram for (a) CeCoIn₅ and (b) CeRhIn₅. At $P \sim P^*$, a non-Fermi liquid (nFL) to Fermi liquid (FL) crossover occurs and T_c reaches a broad maximum. In CeRhIn₅, P_c is a critical pressure which separates the AF metallic and superconducting states, indicating that the AF QCP is located at or in the vicinity of P_c . In CeCoIn₅, the AF QCP appears to be at a slightly negative inaccessible pressure ($P_c < 0$). Arrows indicate the pressures used in this study.

relaxation time approximation) for describing transport experiments on strongly correlated electron systems.²¹ However there is no established explanation for the non-Fermi liquid behavior observed in the basic transport properties. Therefore the anomalous T - and H -dependence of the dc resistivity, Hall effect, and magnetoresistance remains one of the most important unresolved issues in strongly correlated electron systems; and an important outstanding question related to this issue is *whether the anomalous transport properties shown in Eqs. (4)–(6) are specific to high- T_c cuprates or represent universal features in strongly correlated electron systems in the presence of strong AF fluctuations.*

Recently, a new class of heavy fermion compounds have been discovered with the chemical formula CeMIn₅, where M can be either Co, Rh, or Ir.^{22–24} CeMIn₅ crystalizes in a quasi two-dimensional (2D) structure that can be viewed as alternating layers of CeIn₃ and MIn₂ stacked sequentially along the tetragonal c -axis. At ambient pressure, CeCoIn₅ is a superconductor with a transition temperature $T_c = 2.3$ K. The electronic specific heat coefficient γ have been measured to be $\gamma = 300$ mJ/K²mol at T_c . CeIrIn₅ is also a superconductor at ambient pressure with $T_c = 0.4$ K and $\gamma = 680$ mJ/K²mol. CeRhIn₅ is an AF metal with Néel temperature $T_N = 3.8$ K. Above $P_c = 1.6$ GPa, CeRhIn₅ undergoes a superconducting transition, indicating that the AF quantum critical point (QCP) is located at or in the vicinity of P_c . Related to the layered structure, de Haas–van Alphen experiments on CeMIn₅ reveal a corrugated cylindrical Fermi surface.^{25,26} In addition, NMR relaxation rate T_1^{-1} measurements indicate the presence of anisotropic (quasi 2D) AF spin fluctuations in the normal state.^{27,28}

Figures 1 (a) and (b) display the pressure-temperature (P - T) phase diagram for CeCoIn₅ and CeRhIn₅, respectively.^{29–31} The figures show that T_c reaches a broad maximum at characteristic pressures $P^* \sim 1.5$ GPa for CeCoIn₅ and $P^* \sim 2.3$ GPa for CeRhIn₅. Note that it is reasonable to speculate that the AF QCP of

CeCoIn₅ is at a slightly negative pressure. In the region $P < P^*$, non-Fermi liquid behavior is observed in many of the thermodynamic quantities, such as heat capacity,³³ magnetic susceptibility,³⁴ and NMR relaxation rate T_1^{-1} .^{27, 28, 35, 36} On the other hand, at $P > P^*$ the non-Fermi liquid behavior is strongly suppressed and recovery of Fermi liquid behavior is observed. The $P - T$ phase diagram is reminiscent of the phase diagram for high- T_c cuprates around optimal doping.

CeMIn₅ superconductors have attracted great interest in the study of strongly correlated electron systems, since the superconductivity instability in CeMIn₅ occurs in the normal state that exhibits pronounced non-Fermi liquid behavior arising from the proximity of the AF QCP.^{23, 29} Among CeMIn₅ systems, the physical properties of CeCoIn₅ have been investigated most extensively. At ambient pressure, CeCoIn₅ shows the hallmarks of proximity to a magnetic instability in the normal state: the logarithmic divergence of the electronic specific heat coefficient $\gamma \sim \ln T$,^{22, 32, 33} Curie–Weiss-like temperature dependence of the uniform susceptibility $\chi \sim \frac{1}{T+\theta}$,³⁴ and a peculiar T -dependence of $T_1^{-1} \propto T^{\frac{1}{4}}$.^{27, 28, 35} have been attributed to strong AF fluctuations in the vicinity of the QCP. Pronounced non-Fermi liquid behavior is observed in the transport properties, in striking contrast to Eqs. (1)–(3). Below the coherent temperature T_{coh} , which corresponds to the Fermi temperature of f -electrons, down to T_c , T -linear dependent ρ_{xx} , strongly T -dependent $|R_H|$ dramatically increasing with decreasing temperature, and a striking violation of Kohler’s rule in the magnetoresistance have been reported. These unusual properties are markedly pronounced when the system approaches the AF QCP. In addition, the Nernst coefficient ν_H in the normal state of CeCoIn₅ has been reported to be strikingly enhanced by more than three orders of magnitude compared with conventional metals.³⁷

The superconducting state of CeMIn₅ has been reported to be highly unusual. Based on the measurements of specific heat,^{38, 39} thermal conductivity,⁴⁰ NMR relaxation rate,^{35, 36} penetration depth,^{41, 42} and Andreev reflection,^{43, 44} the superconducting gap function of CeCoIn₅ has line nodes and is most likely to have $d_{x^2-y^2}$ -wave symmetry,^{40, 44, 45} indicating an intimate relation between the superconductivity and the AF fluctuations. Thus the phase diagram of CeMIn₅, along with the appearance of the $d_{x^2-y^2}$ -wave superconductivity near the AF ordered state, indicates that CeMIn₅ shares some unconventional properties with high- T_c cuprates. Further, a new pairing state (Fulde-Ferrel-Larkin-Ovchinnikov state) has been suggested at the low- T /high- H corner in the H - T phase diagram of CeCoIn₅.⁴⁶

We stress that the CeMIn₅ system is very suitable for the detailed study of the charge transport properties of strong correlated electron systems, providing a unique opportunity to clarify the universality of transport properties in the presence of strong AF fluctuations, especially when the system is in the vicinity of the QCP. This is because *the electronic structure can be tuned over a wide range continuously from the AF ordered state to*

the Fermi liquid state through the non-Fermi liquid state, by applying pressure without introducing additional scattering centers and with keeping the carrier number unchanged. In addition, CeMIn₅ is in a very clean regime. In fact, the quasiparticle mean free path in the superconducting state of CeCoIn₅ is as long as a few μm .⁴⁷ This is important because the intrinsic transport properties relevant to the electron–electron correlation are often masked by the impurity scattering.

The case for in CeMIn₅ contrastz with the chemical doping in high- T_c cuprates, which always introduces randomness that strongly influences the transport properties. Moreover, in most heavy fermion superconductors, the anomalous Hall term due to skew scattering, which arises from the asymmetric scattering of conduction electrons by the angular momentum of f -electrons, dominates the Hall effect.^{48–50} This effect is strongly temperature dependent and masks the ordinary Hall term arising from the Lorenz force. In contrast to other heavy fermion compounds, the skew scattering term in CeMIn₅ is absent or extremely small.^{51, 52} This allows a detailed analysis of the normal Hall effect to be made.

As well as the non-Fermi liquid behavior of the transport quantities, the evolution of the Fermi surface when crossing the QCP is an important issue in strongly correlated electron systems. Two contrary views have been proposed concerning this evolution. Theories based on spin-density-wave (SDW) predicts a continuous change of the Fermi surface.^{53, 54} On the other hand, theories based on the breakdown of composite Fermions predict a jump of the Fermi surface volume at the QCP.⁴ To help clarify this controversial issue, the importance of Hall measurements, which can probe the Fermi surface, has been highlighted.⁴ Thus CeRhIn₅, which can be tune from AF metal to superconductor, is a suitable system to study the evolution of the Fermi surface.

In this paper, we present systematic studies of the dc-resistivity, Hall effect, and magnetoresistance of CeMIn₅ (M : Co and Rh), ranging from the AF metal state to the Fermi liquid state through the non-Fermi liquid state, using pressure as a tuning parameter. We also show that the transport properties of LaMIn₅, which has a similar band structure but has no f -electron, exhibit typical Fermi liquid behavior as expressed in Eqs. (1)–(3). In sharp contrast, the electron transport properties of CeCoIn₅ and CeRhIn₅ exhibit a striking deviation from Fermi liquid behavior. We analyze these results in accord with the proposed transport theories for non-Fermi liquid behavior in strongly correlated electron systems and compare the results with those for high- T_c cuprates. Several noticeable features commonly observed in high- T_c cuprates and CeCoIn₅ highlight the transport property anomalies in strongly correlated electron systems.

2. Experimental

High quality single crystals of CeRhIn₅, CeCoIn₅, LaRhIn₅, and LaCoIn₅ were grown by the self-flux method. We performed all measurements on samples with typical dimensions of $1.0 \times 2.0 \times 0.05 \text{ mm}^3$ in the

transverse geometry ($\mathbf{H} \parallel c$, $\mathbf{J} \parallel a$). The Hall effect and transverse magnetoresistance were measured simultaneously. We obtained ρ_{xy} from the transverse resistance by subtracting the positive and negative magnetic field data. Hydrostatic pressure up to 2.62 GPa was generated in a piston–cylinder type high pressure cell with oil as a transmitting fluid (Daphne 7373). The pressure inside the cell was determined by the superconducting transition temperature of Pb.

3. Results

3.1 *dc-resistivity*

Figures 2 (a) and (b) depict the temperature dependence of the dc-resistivity ρ_{xx} in zero field under pressure for CeCoIn₅ and CeRhIn₅, respectively. ρ_{xx} of LaCoIn₅ and LaRhIn₅ are also plotted. The overall behavior of CeMIn₅ is typical for Ce-based heavy fermion compounds. In the high temperature regime where the *f*-electrons are well localized, ρ_{xx} increases gradually with decreasing temperature due to the Kondo effect between the conduction electrons and localized *f*-electron spins. Associated with the coherent–incoherent crossover, ρ_{xx} shows a broad maximum around the coherent temperature T_{coh} , and at lower temperatures where the *f*-electrons become itinerant, ρ_{xx} exhibits a metallic temperature dependence.

Figures 2 (c) and (d) depict the magnetic part of the resistivities obtained by subtracting resistivity of LaMIn₅ from ρ_{xx} ; $\rho_{xx}^{mag} \equiv \rho_{xx} - \rho_{xx}(\text{LaMIn}_5)$, plotted as a function of T/T_{coh} in the superconducting regime. Here T_{coh} is defined as the temperature at which ρ_{xx}^{mag} is maximum. The insets of Figs. 2 (c) and (d) show the pressure dependence of T_{coh} . An increase in pressure leads to an increase in T_{coh} and a decrease in ρ_{xx} due to an enhancement of the hybridization between conduction electrons and *f*-electrons through the expansion of the band width of the conduction electrons. On the other hand, T_{coh} decreases with pressure in the AF metal regime of CeRhIn₅ ($P < P_c$ in Fig. 1 (b)).

At ambient pressure, ρ_{xx}^{mag} of CeCoIn₅ displays an almost perfect linear T -dependence below $T \sim T_{coh}/2$ down to T_c . At $P = 2.51$ GPa, however, an apparent deviation from T -linear dependence is seen in ρ_{xx}^{mag} ; the overall T -dependence above T_c up to $T \sim T_{coh}/2$ is well fitted by $\rho_{xx}^{mag} \propto T^\alpha$ with $\alpha \approx 1.2$. For CeRhIn₅, the resistivity shows T -dependence with a convex shape with $\alpha < 1$ above T_c . This behavior is less pronounced as the pressure increases. The fact that the power α in the temperature dependence of the resistivity increases with pressure is an indication that the system approaches the Fermi liquid regime.

3.2 *Hall effect*

Figure 3 (a) depicts the H -dependence of the Hall resistivity ρ_{xy} for CeRhIn₅ at $P = 2.01$ GPa ($P > P_c$). Figures 3 (b) and (c) depict $\rho_{xy}(H)$ for CeCoIn₅ at ambient pressure and at $P = 2.51$ GPa (see Figs. 1 (a) and (b)). The Hall sign is negative for both systems in the present T -, H -, and P -ranges. At low temperatures, ρ_{xy}

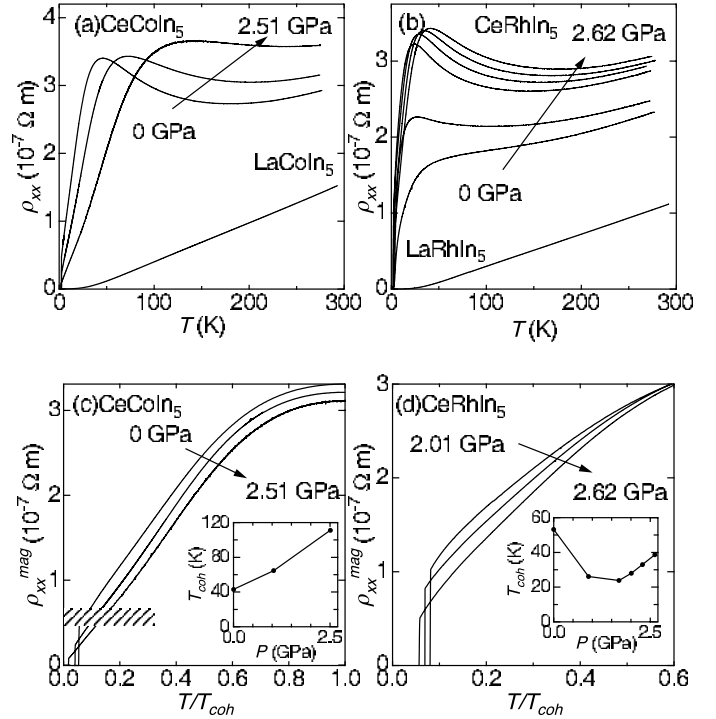


Fig. 2. (a) Temperature dependence of the dc-resistivity ρ_{xx} in zero field of CeCoIn₅ under different pressures, together with the data of LaCoIn₅. (b) The same plot for CeRhIn₅ and LaRhIn₅. (c) Magnetic part of the resistivity, $\rho_{xx}^{mag} = \rho_{xx} - \rho_{xx}(\text{LaCoIn}_5)$, for CeCoIn₅ obtained from (a), plotted as a function of T/T_{coh} . The hatched area indicates the region where R_H is minimum. For detail, see the text (§4.4). Inset: P -dependence of T_{coh} , at which ρ_{xx}^{mag} is maximum, for CeCoIn₅. (d) $\rho_{xx}^{mag} = \rho_{xx} - \rho_{xx}(\text{LaRhIn}_5)$ for CeRhIn₅ obtained from (b), plotted as a function of T/T_{coh} . Inset: P -dependence of T_{coh} for CeRhIn₅.

exhibits a non-linear H -dependence, which is more pronounced when the system approaches the AF QCP.

We first discuss the Hall effect at $P > P_c$ where the system undergoes a superconducting transition. Figures 4 (a) and (b) depict the T -dependence of R_H , defined as the field derivative of ρ_{xy} , $R_H \equiv \frac{d\rho_{xy}}{dH}$, at the zero field limit ($H \rightarrow 0$) for CeRhIn₅ at $P > P_c$ and for CeCoIn₅, respectively. For comparison, R_H for LaRhIn₅ and LaCoIn₅ at ambient pressure is also plotted in Figs. 4 (a) and (b), respectively. Although we do not show it here, ρ_{xy} for both La-compounds show nearly perfect H -linear dependence. With decreasing T , R_H for both La-compounds show a slight increase and the amplitude at low temperature is approximately $-5 \times 10^{-10} \text{ m}^3/\text{C}$, which is nearly half the Hall coefficient expected for one electron per unit cell. This indicates the presence of small hole pockets at the Fermi surface.

Before discussing the Hall effect in CeMIn₅, we recall the Hall effect in other heavy fermion systems. The Hall effect in conventional heavy fermion compounds has been studied extensively and is known to exhibit a similar behavior, irrespective of the system (see Figs. 1 and 2 in Ref. [48]). At high temperatures above T_{coh} , R_H is mostly positive and is much larger than $1/ne$. Below T_{coh} , R_H decreases rapidly with decreasing T after showing a broad maximum at a temperature slightly be-

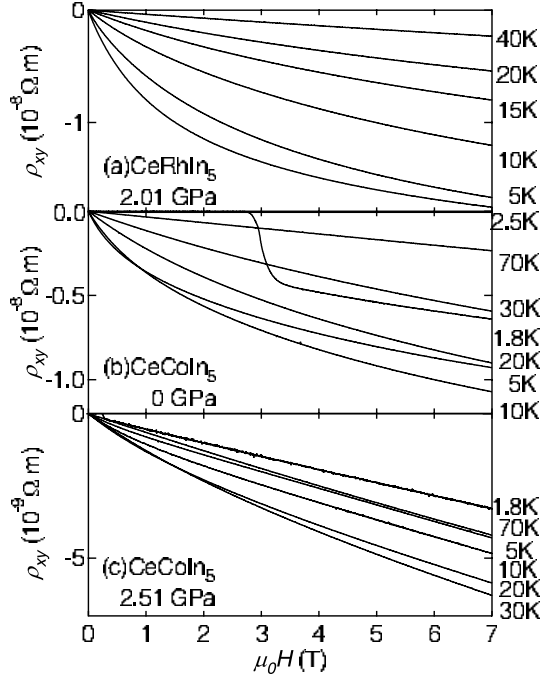


Fig. 3. Field dependence of the Hall resistivity ρ_{xy} for (a) CeRhIn₅ at $P = 2.01$ GPa ($P > P_c$), (b) CeCoIn₅ at ambient pressure, and (c) CeCoIn₅ at $P = 2.51$ GPa.

low T_{coh} . At very low temperature, the amplitude of R_H is strongly reduced and becomes nearly T -independent. This anomalous temperature dependence of R_H can be explained as follows. Generally the Hall effect in heavy fermion system can be decomposed into two terms: $R_H = R_H^n + R_H^a$. Here, R_H^n is the ordinary Hall effect due to the Lorentz force and is nearly T -independent within the Bloch–Boltzmann approximation. Meanwhile, R_H^a represents the so-called “anomalous Hall effect” due to skew scattering, which originates from the assymmetric scattering of the conduction electrons by the angular momenta of f -electrons, induced by the external magnetic field. The sign of R_H^a is positive in almost all Ce-based heavy fermion compounds. This term is strongly temperature-dependent and is well-scaled by the uniform susceptibility: above T_{coh} , R_H^a scales as $R_H^a \propto \chi^{50}$ or $\chi \rho_{xx}$,^{48,49} while below T_{coh} , $R_H^a \propto \chi \rho_{xx}^2$.⁵⁰ The magnitude of R_H^a is much larger than $|R_H^n|$ except at $T \ll T_{coh}$ and $T \gg T_{coh}$, where the contribution of the skew scattering vanishes.

It is obvious that the Hall effect in CeRhIn₅ and CeCoIn₅ shown in Figs. 4 (a) and (b) is distinctly different from those in other heavy fermion systems. The first important signature is that R_H is nearly T -independent in the high temperature regime above T_{coh} and cannot be scaled either by $\chi \rho_{xx}$ or χ , both of which have a strong T -dependence above T_{coh} . In addition, χ is almost strictly H -linear up to 12 T at $T > 2$ K, while ρ_{xy} shows a non-linear H -dependence, as shown in Figs. 3 (a), (b), and (c). Moreover, the amplitude of R_H above T_{coh} is much smaller than those of other heavy fermion systems above T_{coh} . Thus, the sign, amplitude, and T -dependence of R_H of CeRhIn₅ and CeCoIn₅ are clearly in conflict with the conventional skew scattering mechanism. These results

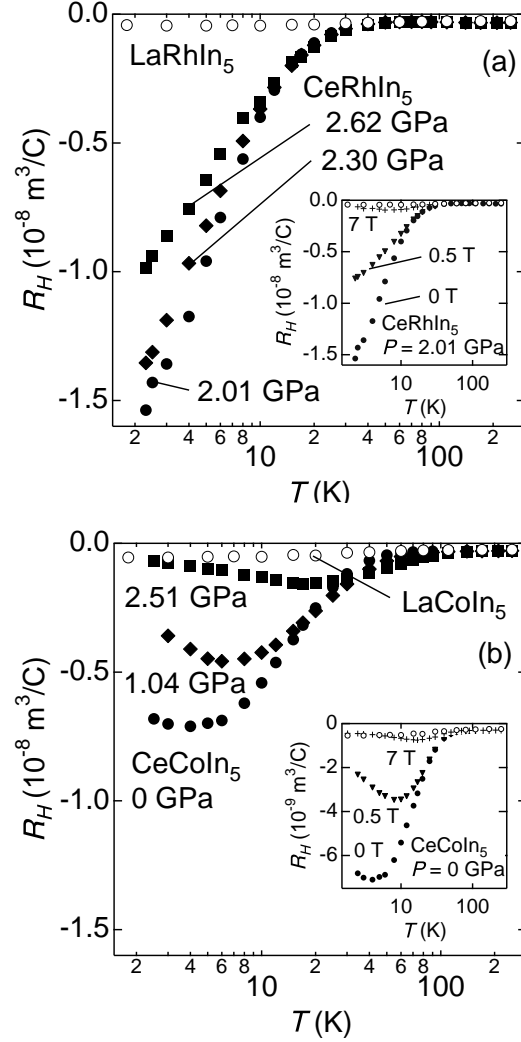


Fig. 4. (a) Temperature dependence of R_H for CeRhIn₅ in the superconducting regime at $P > P_c$, $P = 2.01$ (●), 2.30 (◆), and 2.62 GPa (■) at the zero field limit, $\lim_{H \rightarrow 0} \frac{d\rho_{xy}}{dH}$, and for LaRhIn₅ at $P = 0$ (○). Inset: The same data for CeRhIn₅ at $P = 2.01$ GPa at $\mu_0 H = 0$ T (●), 0.5 T (▼), and 7 T (+), defined as $d\rho_{xy}/dH$, and for LaRhIn₅ (○). (b) Temperature dependence of R_H for CeCoIn₅ at $P = 0$ (●), 1.04 (◆), and 2.51 GPa (■) at the zero field limit, $\lim_{H \rightarrow 0} \frac{d\rho_{xy}}{dH}$, and for LaCoIn₅ (○). Inset: The same data for CeCoIn₅ at ambient pressure at $\mu_0 H = 0$ T (●), 0.5 T (▼), and 7 T (+), defined as $d\rho_{xy}/dH$, and for LaCoIn₅ (○).

prove that skew scattering in CeRhIn₅ and CeCoIn₅ is negligibly small and that R_H is dominated by the normal part of the Hall effect. At present, it is not clear why skew scattering is absent in CeMIn₅ is not clear and a theoretical study based on realistic p - f model for CeMIn₅ would be required to clarify this point. The absence of skew scattering enables us to analyze the normal Hall effect R_H^n in detail.

In both CeRhIn₅ and CeCoIn₅, the temperature dependence of the Hall effect is closely correlated with that of the resistivity. At high temperatures $T > T_{coh}$, R_H at all pressures in CeMIn₅ is nearly independent of temperature and coincides well with R_H of LaMIn₅, *i.e.* $R_H \sim 1/ne$. This is consistent with band structure cal-

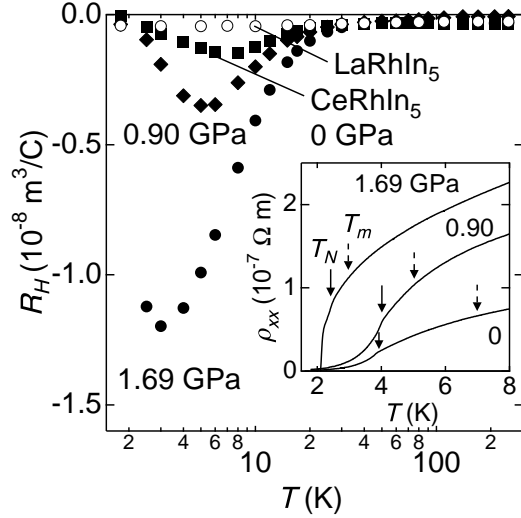


Fig. 5. Main panel: Temperature dependence of R_H for CeRhIn₅ in the AF metallic regime at $P < P_c$, $P = 1.69$ (●), 0.90 (◆), and 0 GPa (■) at the zero field limit, and for LaRhIn₅ at $P = 0$ (○). Inset: Temperature dependence of the dc-resistivity for CeRhIn₅ in the AF metallic regime. Solid arrows indicate the Néel temperature. Dashed arrows indicate the temperature at which the amplitude of R_H is maximum.

culations, which predict that the electronic structure of CeMIn₅ is similar to that of LaMIn₅. Therefore it is natural to assume that R_H of LaMIn₅ is close to the Hall coefficient in the Fermi liquid limit of CeMIn₅. Below T_{coh} , the carrier number of CeMIn₅ is expected to slightly increase from that of LaMIn₅, since the f -electrons participate in the conduction.

Below T_{coh} , R_H of both CeRhIn₅ and CeCoIn₅ exhibits a remarkable departure from R_H of LaRhIn₅ and LaCoIn₅, respectively; the amplitude of R_H increases rapidly below T_{coh} at all pressures as the temperature is lowered. At very low temperatures, the behavior of R_H is

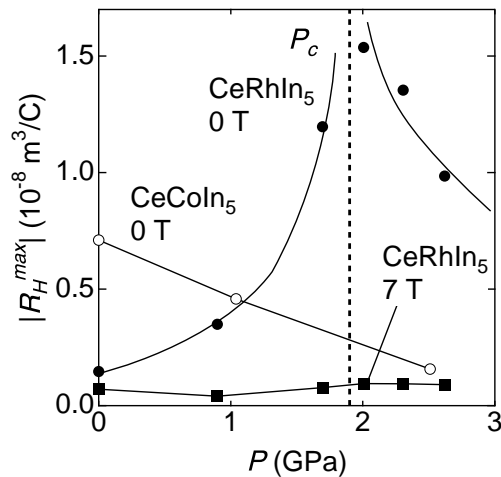


Fig. 6. Maximum of $|R_H|$ vs. pressure for CeRhIn₅ at $\mu_0 H = 0$ T (●), and 7 T (■) and for CeCoIn₅ at $\mu_0 H = 0$ T (○). At P_c , $|R_H|$ of CeRhIn₅ at 0 T exhibits a divergent behavior.

different for both CeRhIn₅ and CeCoIn₅. In CeRhIn₅, as shown in Fig. 4 (a), the amplitude of R_H increases monotonically down to T_c . Below T_c , the Hall signal vanishes. At $P = 2.01$ GPa, slightly above P_c , the amplitude of R_H is strikingly enhanced below T_{coh} ; the amplitude of R_H just above T_c is enhanced to nearly 50 times that at high temperatures above T_{coh} , which is $\sim |1/ne|$. On the other hand, in CeCoIn₅, R_H exhibits an upturn at low temperatures; the amplitude of R_H decreases after showing a maximum at around $T = 4, 6,$ and 20 K for $P = 0, 1.04,$ and 2.51 GPa, respectively. At ambient pressure, the amplitude of R_H at low temperatures is enhanced to nearly 30 times that above T_{coh} . In both CeRhIn₅ and CeCoIn₅, the low temperature enhancement of the amplitude of R_H is dramatically suppressed in the high pressure regime where non-Fermi liquid behavior is suppressed. Interestingly, R_H of CeCoIn₅ at $P = 2.51$ GPa approaches R_H of LaCoIn₅, *i.e.* the Fermi liquid value, at very low temperatures.

We next discuss the Hall effect of CeRhIn₅ in the AF metallic regime at $P < P_c$ (see Fig. 1 (b)). Figure 5 shows the T -dependence of R_H . Below T_{coh} , as the temperature is lowered, the amplitude of R_H increases rapidly and then decreases after a maximum at ~ 3 K, ~ 5 K, and ~ 7 K for $P = 1.69, 0.90$ and 0 GPa, respectively. This behavior is similar to that for CeCoIn₅ shown in Fig. 4 (b). The inset of Fig. 5 depicts the T -dependence of ρ_{xx} at low temperatures. Below the Néel temperature T_N , shown by solid arrows, ρ_{xx} varies as T^2 , indicating Fermi liquid behavior. The dashed arrows indicate the temperature at which the amplitude of R_H is maximum. These temperatures are located well above T_N .

Thus there are three distinct T -regions in the Hall effect: high- T -region, where R_H is nearly T -independent; intermediate- T -region, where the amplitude of R_H increases rapidly; and low- T -region, where the amplitude of R_H begins to decrease. (A schematic figure of R_H is illustrated in Fig. 13. We denote the three regions as region-(I), (II), and (III).) The low- T -region is absent in CeRhIn₅ in the superconducting region at $P > P_c$. We will discuss the behavior of the Hall effect in the low- T -region in a later section.

In Fig. 6, we plot the P -dependence of the maximum values of $|R_H|$, $|R_H^{\max}|$, obtained from Figs. 4 (a) and (b) and Fig. 5. For CeRhIn₅, $|R_H^{\max}|$ at $\mu_0 H \rightarrow 0$ T increases rapidly as P_c is approached from either the AF metallic ($P < P_c$) or superconducting ($P > P_c$) regimes. At $\mu_0 H = 7$ T, $|R_H^{\max}|$ exhibits a maximum at a pressure slightly higher than P_c . We will discuss this behavior later. For CeCoIn₅ with negative P_c , $|R_H^{\max}|$ increases as P_c is approached. *These results provide direct evidence that the Hall effect is strongly influenced by the AF fluctuations associated with the AF QCP.*

It has been argued that in high- T_c cuprates, the Hall problem can be simplified when analyzed in terms of the cotangent of the Hall angle $\cot \Theta_H$.^{11–13,20} A very recent systematic study of R_H on La_{2–x}Sr_xCuO₄ single crystals over a wide doping range has shown that the T^2 -law of $\cot \Theta_H$ holds well from the underdoped region up to optimal doping, but gradually breaks down, showing a neg-

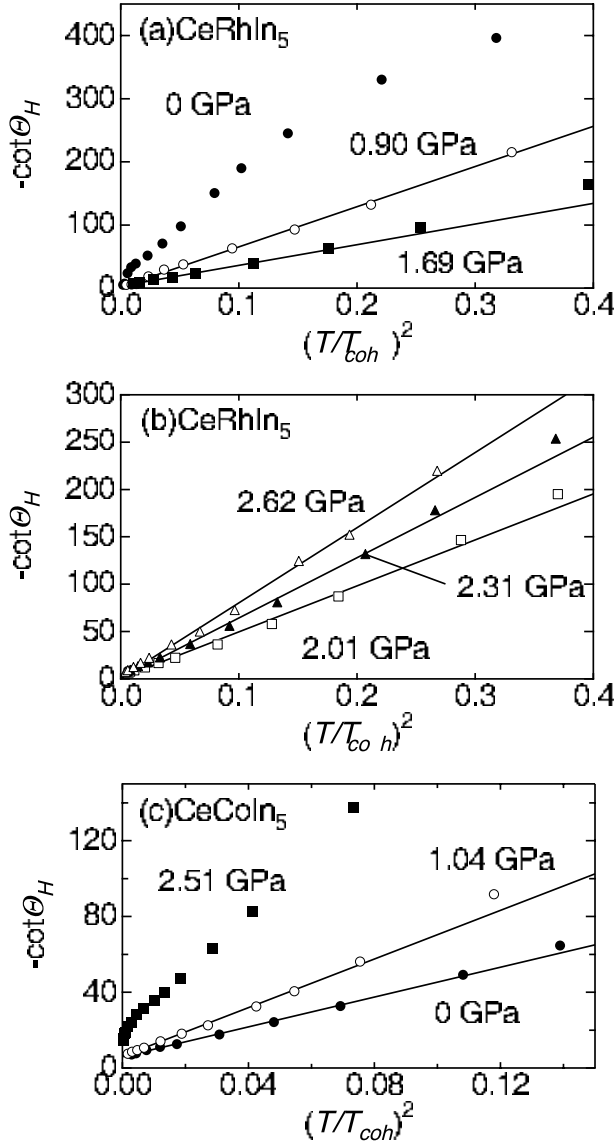


Fig. 7. $-\cot \Theta_H$ versus T/T_{coh} for (a) CeRhIn₅ in the AF metallic regime ($P < P_c$), (b) CeRhIn₅ in the superconducting regime ($P > P_c$), and (c) CeCoIn₅, at different pressures. The solid lines represent the T^2 -dependence of $\cot \Theta_H$.

ative curvature when the system is overdoped.¹¹ We here examine the pressure dependence of $\cot \Theta_H$ for CeRhIn₅ and CeCoIn₅. Figures 7 (a) and (b) depict $\cot \Theta_H$ for CeRhIn₅ at $P < P_c$ and $P > P_c$, respectively. We plot the data as a function of $(T/T_{coh})^2$. Figure 7 (c) shows the same plot for CeCoIn₅. As seen from the solid lines in these figures, $\cot \Theta_H$ obeys a T^2 -dependence near the AF QCP. On the other hand, $\cot \Theta_H$ apparently deviates from the T^2 -law with a negative curvature, as shown for CeCoIn₅ at $P = 2.51$ GPa in the regime where the non-Fermi liquid behavior is less pronounced. This behavior is similar to overdoped La_{2-x}Sr_xCuO₄. For CeRhIn₅ at ambient pressure, deviation from the T^2 -law is also observed.

We here comment on the recent consideration of R_H in CeCoIn₅ in terms of the two-fluid Kondo model, in which the Kondo lattice system is divided into coherent and incoherent parts. It has been proposed that R_H

can be expressed as $R_H = \alpha_f R_H^{La}$, where α_f is the f -electron weighting function reflecting the coherent part.⁵⁵ However, if we apply this model to R_H at 2.51 GPa, α_f is close to unity at low temperatures, indicating that there is no coherent part. This is not consistent with itinerant f -electrons in this temperature regime. Therefore the two-fluid Kondo scenario appears to be inconsistent with the present results.

3.3 Magnetoresistance

Figure 8 (a) displays the magnetoresistance $\Delta\rho_{xx}/\rho_{xx}$ at various temperatures for CeRhIn₅ at $P = 2.01$ GPa ($P > P_c$). The same plot for CeCoIn₅ at $P = 0$ and 2.51 GPa is shown in Figs. 8 (b) and (c), respectively. The magnetoresistance is positive at low fields for both compounds. The magnetoresistance exhibits H^2 -dependence at very low fields; for CeCoIn₅ at ambient pressure, this field range is less than 0.1 T. For CeRhIn₅ at 2.01 GPa and CeCoIn₅ at ambient pressure, where the system is close to the AF QCP, the resistivity shows H -dependence with a concave downward shape at low temperatures. At ambient pressure for CeCoIn₅, the slope of the magnetoresistance turns from positive to negative at high fields below 5 K. This crossover field increases with temperature. The magnitude of the low field positive magnetoresistance decrease with temperature. The origin of high field negative magnetoresistance is possibly due to suppression of spin-flop scattering by the magnetic field, which is often observed in conventional heavy fermion compounds below T_{coh} . In this paper, we will address the low field magnetoresistance.

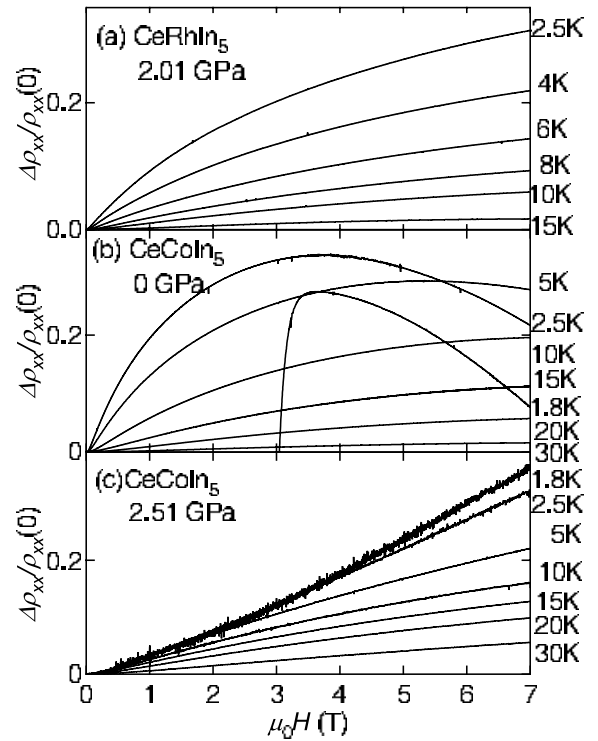


Fig. 8. Magnetoresistance $\Delta\rho_{xx}/\rho_{xx}$ at different temperatures for (a) CeRhIn₅ at $P = 2.01$ GPa ($P > P_c$), (b) CeCoIn₅ at ambient pressure, and (c) CeCoIn₅ at $P = 2.51$ GPa.

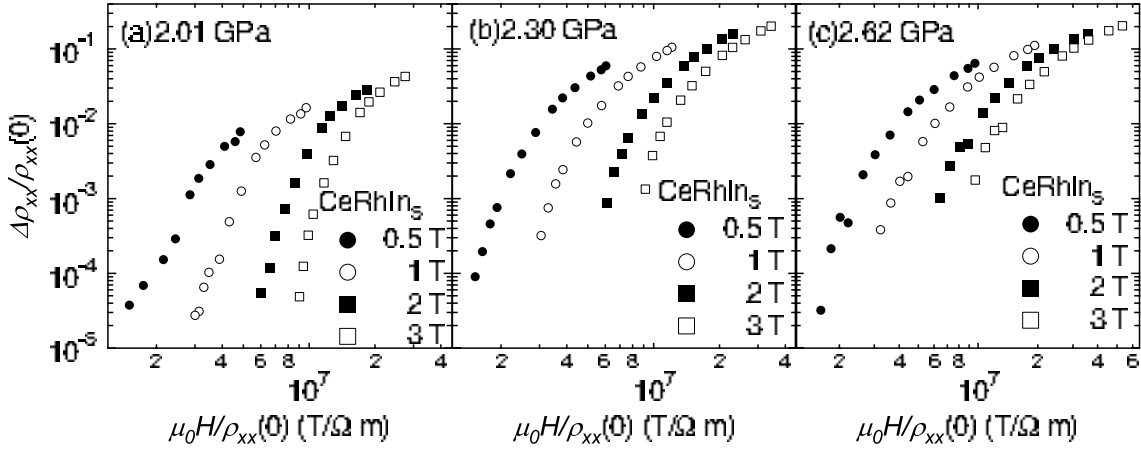


Fig. 10. Kohler's plot: $\Delta\rho_{xx}/\rho_{xx}$ versus μ_0H/ρ_{xx} for CeRhIn₅ in the superconducting regime ($P > P_c$) at (a) $P = 2.01$, (b) 2.30, and (c) 2.62 GPa. Apparent violation of Kohler's rule is observed at all pressures.

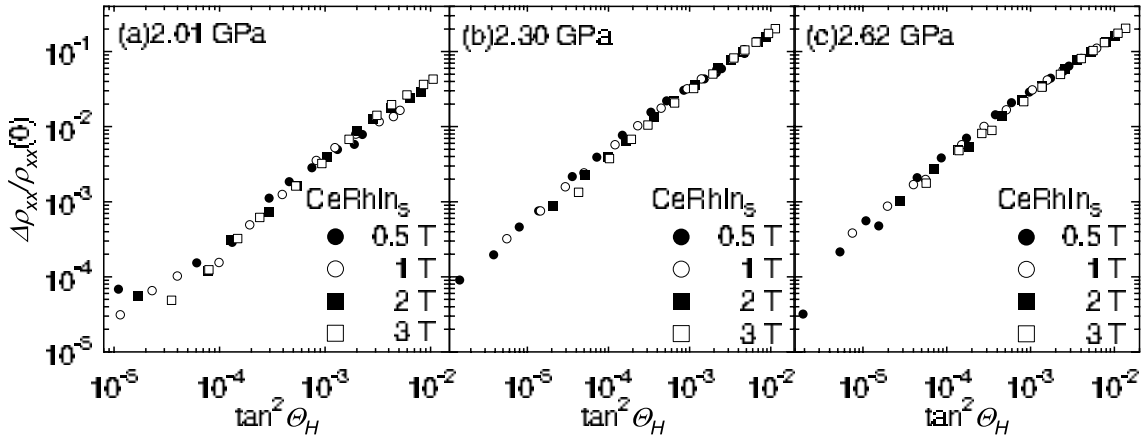


Fig. 11. $\Delta\rho_{xx}/\rho_{xx}$ plotted as a function of $\tan^2\Theta_H$ for CeRhIn₅ in the superconducting regime ($P > P_c$) at (a) $P = 2.01$, (b) 2.30, and (c) 2.62 GPa. At all pressures, the magnetoresistance at different fields collapses into the same curves for four orders of magnitude in $\Delta\rho_{xx}/\rho_{xx}(0)$, indicating the applicability of the modified Kohler's rule shown in Eq. (6).

In conventional metals, a positive magnetoresistance usually obeys Kohler's rule, a scaling relation described by Eq. (3). Violation of Kohler's rule is sometimes observed even in conventional metals when the Fermi surface is composed of multiple bands and the carrier scattering rate is strongly band dependent.² To examine Kohler's rule in the present systems, it is necessary to extract the orbital part of the magnetoresistance. Usually, for this purpose, the longitudinal magnetoresistance measured in the geometry $\mathbf{H} \parallel \mathbf{J} \parallel a$ is subtracted from the transverse magnetoresistance. However, in a material with a 3D Fermi surface, the orbital magnetoresistance appears even in the longitudinal geometry.⁵⁶ We therefore assume that the transverse magnetoresistance is dominated by the orbital components in the present materials. To check this, we test Kohler's rule for LaRhIn₅, which has a similar band structure as CeRhIn₅. Figure 9 displays Kohler's plot for LaRhIn₅; $\Delta\rho_{xx}/\rho_{xx}(0)$ plotted as a function of $\mu_0H/\rho_{xx}(0)$. $\Delta\rho_{xx}/\rho_{xx}(0)$ at different fields collapses into the same curve for four orders of magnitude as a function of $\mu_0H/\rho_{xx}(0)$, indicating that the magnetoresistance obeys the Kohler's rule

in Eq. (3) quite well. We obtained similar results for LaCoIn₅. These results indicate the validity of the assumptions that the multiband effect is not important and the transverse magnetoresistance is dominated by orbital effects.

Figures 10 (a), (b), and (c) shows Kohler's plots for CeRhIn₅ at $P = 2.01$, 2.30, and 2.62 GPa ($P > P_c$ in Fig. 1 (b)), respectively. In sharp contrast to LaRhIn₅, $\Delta\rho_{xx}/\rho_{xx}(0)$ at different fields are on distinctly different curves, indicating apparent violation of Kohler's rule. We next examine the data in accordance with Eq. (6), which has shown to describe well the magnetoresistance in high- T_c cuprates.¹⁴ Figures 11 (a), (b), and (c) display the magnetoresistance as a function of $\tan^2\Theta_H$. *At all pressures, the magnetoresistance data at different fields collapse into the same curves for four orders of magnitude in $\Delta\rho_{xx}/\rho_{xx}(0)$.* Although we do not show it here, we obtained essentially the same results for CeCoIn₅. Thus in the pressure regime where non-Fermi liquid behavior is pronounced in CeCoIn₅ and CeRhIn₅, the magnetoresistance exhibits a striking violation of Kohler's rule in Eq. (3), while the magnetoresis-

tance obeys the scaling relation expressed by Eq. (6) quite well.

Interestingly, both violation and nonviolation of Kohler's rule can be seen simultaneously in the AF metal regime ($P < P_c$) of CeRhIn₅, as shown in Fig. 12. The solid and open circles represent the data above and below T_N . As shown in the inset of Fig. 5, ρ_{xx} exhibits Fermi liquid behavior below T_N , while non-Fermi liquid behavior is observed in ρ_{xx} above T_N . The magnetoresistance well obeys Kohler's rule below T_N , while violation of Kohler's rule is observed above T_N . These results reinforce the conclusion that Kohler's rule is violated only in the regime where non-Fermi liquid behavior is observed.

4. Discussion

4.1 Striking resemblance between CeMIn₅ and high- T_c cuprates

Summarizing the non-Fermi liquid behavior observed in the transport properties of CeMIn₅ below the Fermi temperature of f -electrons T_{coh} ,

- (1) The dc-resistivity shows T -linear dependence, $\rho_{xx} \propto T$, over a wide temperature range below T_{coh} down to T_c .
- (2) Below T_{coh} , $|R_H|$ increases rapidly with decreasing temperature, depending on T as $R_H \propto 1/T$, and reaches a value much larger than $|1/ne|$ at low temperatures. The cotangent of the Hall angle varies as $\cot \Theta_H \propto T^2$.
- (3) The magnetoresistance displays T - and H -dependence that strongly violate Kohler's rule, and is well scaled by the tangent of the Hall angle: $\Delta\rho_{xx}/\rho_{xx} \propto \tan^2 \Theta_H$.

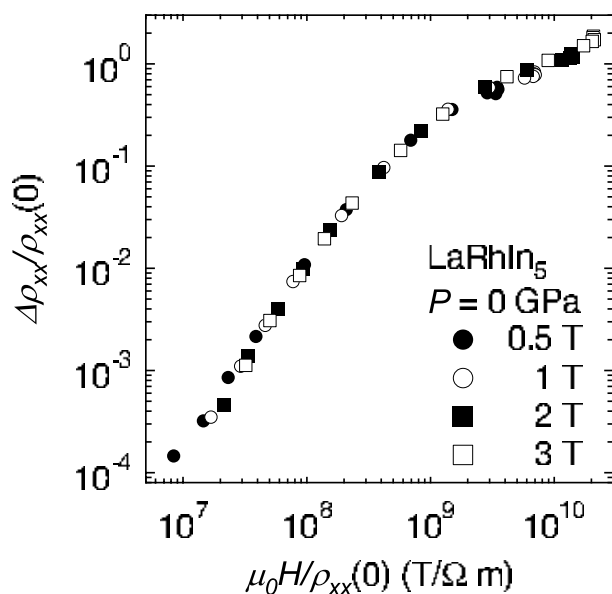


Fig. 9. Kohler's plot: $\Delta\rho_{xx}/\rho_{xx}$ versus $\mu_0 H/\rho_{xx}$ for LaRhIn₅ at ambient pressure. $\Delta\rho_{xx}/\rho_{xx}$ at different fields collapses into the same curve for four orders of magnitude, indicating the applicability of the Kohler's rule shown in Eq. (3)

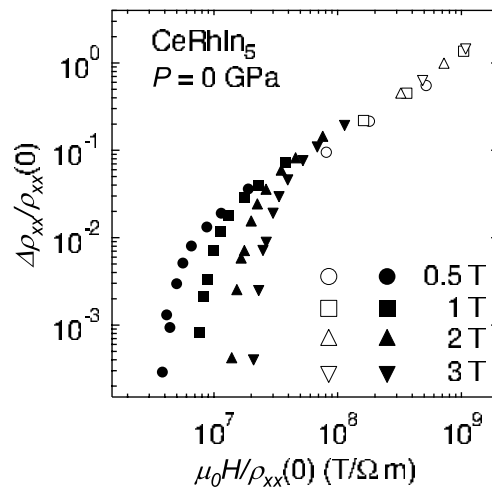


Fig. 12. Kohler's plot, $\Delta\rho_{xx}/\rho_{xx}$ versus $\mu_0 H/\rho_{xx}$ in the AF metal regime ($P < P_c$) of CeRhIn₅. The solid and open circles represent the data above and below T_N . Kohler's rule is satisfied below T_N , where the resistivity shows a Fermi liquid behavior, shown in the inset of Fig. 5. In sharp contrast violation of Kohler's rule is observed above T_N , where non-Fermi liquid behavior is observed in the resistivity.

We emphasize that all of these salient features have been reported for high- T_c cuprates, as discussed in §1. *The striking resemblance between high- T_c cuprates and CeMIn₅ lead us to consider that the anomalous transport properties in both systems originate from the same mechanism.* It should be noted that in high- T_c cuprates the presence of the pseudogap in the underdoped regime reduces both R_H and ρ_{xx} , while the presence of the pseudogap at $P < P^*$ in CeCoIn₅ is controversial.²⁹ Since the anomalous transport behavior seem to present an insurmountable challenge to the Fermi liquid theory, several notable attempts to explain these behavior have been made for high- T_c cuprates. Two broad approaches have been proposed to understand the transport properties in high- T_c cuprates: non-Fermi liquid and Fermi liquid approaches.

In models based on a non-Fermi liquid ground state, it is proposed that the transport carriers are exotic objects, such as spinons and holons that may model the doped CuO₂ 2D planes.¹²⁻¹⁴ This model involves two distinct relaxation times for momentum changes parallel and perpendicular to the Fermi surface, associated with spin-charge separation. It has been argued that the T -linear ρ_{xx} and the T^2 -dependence of $\cot \Theta_H$ imply the existence of different longitudinal and Hall relaxation rates that change as $\tau_{tr} \propto T$ and $\tau_H \propto T^2$, respectively. Then, the diagonal conductivity, Hall conductivity, and magnetoresistance depend on τ_H and τ_{tr} as $\sigma_{xx} \propto \tau_{tr}$, $\sigma_{xy} \propto \tau_H \tau_{tr}$, and $\Delta\rho_{xx}/\rho_{xx} \propto \tau_H^{-2}$, respectively, which can reproduce the data. However this idea of scattering rate separation has not yet gained complete consensus. It should be noted that the parent material of high- T_c cuprates is a Mott insulator, while that of CeMIn₅ is an AF metal. Moreover, the anisotropy of the electronic structure of CeMIn₅ is not large compared with high- T_c

cuprates; the anisotropy ratio of the Fermi velocity parallel and perpendicular to the ab -plane, v_{\parallel}/v_{\perp} , is more than 100 for high- T_c cuprates, while it is ~ 2 for CeMIn_5 . Therefore it seems highly unlikely that spin–charge separation in the 2D plane discussed in relation to cuprates is realized in CeRhIn_5 and CeCoIn_5 .

In the Fermi liquid approach, a strong anisotropy of the transport scattering rate arising from the coupling to a singular bosonic mode, such as AF spin fluctuations, is assumed.^{16–20} Since the anomalous features in the magnetotransport properties are more pronounced when the system approaches the AF QCP, as shown by the P -dependence of R_H in Figs. 4 (a) and (b), it is natural to consider that the AF fluctuations play an essential role in determining the electron transport coefficients. The H -dependence of R_H provides strong support for this idea. As indicated by resistivity,⁵⁷ heat capacity,³³ magnetization,³⁴ and NMR relaxation rate³⁶ measurements, AF fluctuations are dramatically suppressed by the magnetic field, and recovery of Fermi liquid behavior is observed above ~ 5 T ($\sim \mu_0 H_{c2}$) for $H \perp ab$ -plane.^{33, 57} The insets of Figs. 4 (a) and (b) show the H -dependence of $R_H = d\rho_{xy}/dH$ of CeRhIn_5 and CeCoIn_5 , respectively. With increasing H , the amplitude of R_H decreases rapidly and approaches R_H of LaMIn_5 . At $\mu_0 H = 7$ T, where the system exhibits Fermi liquid behavior, R_H is very close to R_H of LaMIn_5 . Thus both the P - and H -dependence of R_H imply that AF fluctuations govern the electron transport phenomena below T_{coh} , particularly in the regime where non-Fermi liquid behavior is observed.

The central concept behind the Fermi liquid approach is the “hot spot”, a small area on the Fermi surface where the electron lifetime is unusually short. Hot spots appear as a result of scattering of the electrons by AF fluctuations. They are located at positions where the AF Brillouin zone intersects the Fermi surface. The presence of hot spots has been confirmed in high- T_c cuprates. It has been reported in CeIn_3 as well, which is a relative compound of CeMIn_5 , by de Haas–van Alphen measurements.⁵⁸ Since the hot spot area does not contribute to the electron transport, it reduces the effective carrier density, which results in enhancement of the amplitude of R_H above $|1/ne|$. However, we note that the Hall effect and magnetoresistance in CeMIn_5 cannot be quantitatively accounted for by Bloch–Boltzmann approaches assuming the presence of hot spots. In fact, according to Ref. [16], R_H can be written as

$$R_H = \frac{1}{en} \frac{1+r}{2\sqrt{r}}, \quad (7)$$

where r is the anisotropy ratio of the scattering time at the hot and cold (non-hot) spots, $r \equiv \tau_{cold}/\tau_{hot}$. Applying this theory to CeRhIn_5 and CeCoIn_5 yields an extremely large r : $r \sim 10000$ for CeRhIn_5 and $r \sim 2500$ for CeCoIn_5 . Such an extremely large anisotropic scattering rate on the Fermi surface is unphysical and inconsistent with some aspects of the experimental data. For instance, such a large r would produce an extremely large magnetoresistance,¹⁷ $\Delta\rho_{xx}/\rho_{xx} \sim 10r \tan^2 \Theta_H > 100$ at 1 T, which is two orders of magnitude larger than the experimental results

shown in Fig. 8.

4.2 Anomalous enhancement of the Hall coefficient

Figure 13 presents a schematic illustration of the T -dependence of R_H for CeCoIn_5 and CeRhIn_5 . There are three distinct T -regions: high- T -region (III), where R_H is nearly T -independent and $|R_H| \sim |1/ne|$; intermediate- T -region (II), where the amplitude of R_H exhibits a rapid increase; and a low- T -region (I), where the amplitude of R_H decreases. Region-(I) is absent in the superconducting regime of CeRhIn_5 at $P > P_c$, as shown in Fig. 4 (a). In region-(III), phonon and incoherent Kondo scattering determine the elastic scattering time τ_e . We here address the enhancement of the amplitude of R_H in region-(II).

Given the failure of the Fermi liquid approach based on the Bloch–Boltzmann approximation to explain the Hall behavior in region-(II), it has been suggested that the approach should be substantially modified due to the backflow effect arising from strong electron correlation.¹⁸ The existence of backflow is a consequence of the charge conservation law, which is intimately related to the transport phenomena. Consequently, neglect of backflow often leads to various unphysical results. In general, backflow is not negligible in strongly correlated systems such as high- T_c cuprates and heavy fermion systems. The backflow is called the current vertex correction in microscopic Fermi liquid theory.

We here attempt to explain the non-Fermi liquid like behavior in the transport properties of CeRhIn_5 and CeCoIn_5 in accordance with theory in which the backflow effect is taken into account. Backflow is explained as follows. According to the Landau-Fermi liquid theory, the energy of a quasiparticle with a wave-vector \mathbf{k} is given by $\tilde{\varepsilon}_{\mathbf{k}} = \varepsilon_{\mathbf{k}} + \sum_{\mathbf{k}'} f(\mathbf{k}, \mathbf{k}') \delta n_{\mathbf{k}'}$, where $\varepsilon_{\mathbf{k}} = \hbar^2 \mathbf{k}^2 / 2m^*$, and m^* is the renormalized mass. $\delta n_{\mathbf{k}}$ is the deviation of a quasiparticle distribution function from the ground state and $f(\mathbf{k}, \mathbf{k}')$ is the Landau interaction function, which stems from electron–electron correlations. Therefore, whole the Fermi surface becomes unstable even if an excited quasiparticle exists. Then, unstable Fermi surface induces excess current, which is called the backflow.⁵⁹

The total current in the collisionless limit ($\omega\tau \gg 1$) is given by

$$\begin{aligned} \mathbf{J}_{\mathbf{k}} &\equiv ne \nabla_{\mathbf{k}} \tilde{\varepsilon}_{\mathbf{k}} \\ &= ne \mathbf{v}_{\mathbf{k}} + ne N(0) \int_{\text{FS}} dk'_{\parallel} f(\mathbf{k}, \mathbf{k}') \mathbf{v}_{\mathbf{k}'}, \end{aligned} \quad (8)$$

where $\mathbf{v}_{\mathbf{k}} = \hbar \mathbf{k} / m^*$ is the renormalized Fermi velocity and the second term represents the backflow. n is the density of electrons, and $N(0)$ is the density of states at the Fermi level. In a spherical system, $\mathbf{J}_{\mathbf{k}}$ is given by $\hbar \mathbf{k} / m$ due to the Galilean invariance of the system. Although $|\mathbf{J}_{\mathbf{k}}|$ is greater than $|\mathbf{v}_{\mathbf{k}}|$ due to backflow, $\mathbf{J}_{\mathbf{k}}$ is parallel to $\mathbf{v}_{\mathbf{k}}$. In anisotropic systems, however, $\mathbf{J}_{\mathbf{k}}$ is not always parallel to $\mathbf{v}_{\mathbf{k}}$, which can modify the Hall coefficient significantly. We stress that the dc conductivity is given by the total current in the hydrostatic limit ($\omega\tau \ll 1$), which is not as same as Eq. (8).¹⁸ Although the effect of backflow is more prominent in the hydro-

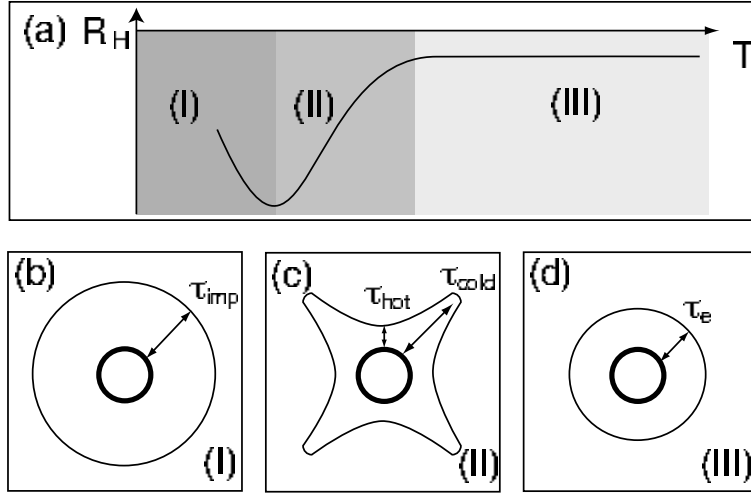


Fig. 13. (a) Schematic figure of the T -dependence of R_H for CeCoIn₅ and CeRhIn₅. There are three distinct T -regions: high- T -region (III), where R_H is nearly T -independent; intermediate- T -region (II), where R_H exhibits a rapid decrease with decreasing T ; and low- T -region (I), where R_H increases. (b), (c), and (d) show the anisotropy of the scattering time $\tau(\phi)$ (thin solid lines) around the Fermi surface (solid lines) at region-(I), (II), and (III), respectively. In region-(II), the scattering time is highly anisotropic, possibly due to AF spin fluctuations. On the other hand, the scattering time is isotropic in region-(I) where impurity scattering dominates and in region-(III) where phonon and incoherent Kondo scattering determine the elastic scattering time τ_e .

static limit, we use Eq. (8) hereafter for simplicity. For the detailed argument, see Ref. [60].

Here we assume a 2D system for simplicity. In the framework of the Bloch–Boltzmann approximation, the Hall conductivity is expressed as

$$\sigma_{xy} = (e^3/2\pi\hbar^2)A_\ell, \quad (9)$$

where A_ℓ^v is the area swept out by the vector ℓ_k^v ($\parallel \mathbf{v}_k$) as \mathbf{k} moves around the Fermi surface given as

$$A_\ell^v = \frac{\mathbf{B}}{2} \cdot \int d\ell_k^v \times \ell_k^v. \quad (10)$$

Here, $\ell_k^v = \mathbf{v}_k \tau_k$ is the mean free path and $\mathbf{v}_k = \partial \epsilon_k / \partial (\hbar \mathbf{k})$ is the Fermi velocity at \mathbf{k} .⁶² However, in the presence of the backflow effect, \mathbf{J}_k is no longer parallel to \mathbf{v} and hence is not perpendicular to the Fermi surface. Therefore, backflow leads to a significant modification of the Hall coefficient and magnetoresistance from the Bloch–Boltzmann value. Figures 14 (a), (b), and (c) schematically show the backflow effect. In the presence of strong AF fluctuation, $f(\mathbf{k}, \mathbf{k}')$ is proportional to the spin susceptibility $\chi(\mathbf{k} - \mathbf{k}')$. Therefore, according to Eq. (8), the backflow is proportional to \mathbf{v}_{k+Q} , where \mathbf{Q} is the AF nesting vector. Then, the total current is approximately proportional to $\mathbf{v}_k + \mathbf{v}_{k+Q}$.

We now consider the “effective Fermi surface” perpendicular to \mathbf{J}_k , which is illustrated in Fig. 14 (b). When \mathbf{J}_k is not parallel to \mathbf{v}_k , A_ℓ^v is replaced by the area swept out by $\ell_k^J = \mathbf{J}_k \tau_k / ne$, as shown in Fig. 14 (c),

$$A_\ell^J = \frac{\mathbf{B}}{2} \cdot \int d\ell_k^J \times \ell_k^J. \quad (11)$$

Around the cold spot, the curvature of the effective Fermi surface is strongly enhanced. Then, the swept area with respect to \mathbf{J}_k can be strongly enhanced, compared with that with respect to \mathbf{v}_k ($A_\ell^J \gg A_\ell^v$). Thus the backflow effect leads to a significant enhancement of the Hall coefficient.

We next discuss the transport coefficient in the presence of the backflow effect in more detail. In the presence of strong anisotropy of the scattering rate at the Fermi surface, various transport properties are determined by τ_{cold} . According to Ref. [18], transport properties under a magnetic field are also governed by the AF correlation length ξ_{AF} in the presence of the backflow effect. In this case, the zero-field diagonal conductivity $\sigma_{xx}(0)$, Hall conductivity σ_{xy} ,¹⁸ and magnetoconductivity $\Delta\sigma_{xx}(H) \equiv \sigma_{xx}(H) - \sigma_{xx}(0)$ ⁶³ are given as

$$\sigma_{xx}(0) \sim \tau_{\text{cold}}, \quad (12)$$

$$\sigma_{xy} \sim \xi_{AF}^2 \tau_{\text{cold}}^2 H, \quad (13)$$

and

$$\Delta\sigma_{xx} \sim \xi_{AF}^4 \tau_{\text{cold}}^3 H^2. \quad (14)$$

Here we note that the non-linearity of σ_{xy} with respect to H is not due to the higher order terms with respect to $H\tau$ because $\omega_c \tau \ll 1$. ($\omega_c = e\mu_0 H/m$ being the cyclotron frequency.) Near the AF QCP, ξ_{AF} depends on T as $\xi_{AF}^2 \propto 1/(T + \theta)$,⁶¹ where θ is the Weiss temperature. Moreover, according to AF spin fluctuation theory, τ_{cold} is nearly inversely proportional to T : $\tau_{\text{cold}} \propto 1/T$.¹⁸ We then obtain the temperature dependence of the resistivity $\rho_{xx} = \sigma_{xx}^{-1}$, Hall coefficient $R_H = \sigma_{xy}/\sigma_{xx}^2 \mu_0 H$, and Hall angle as

$$\rho_{xx} \propto \tau_{\text{cold}}^{-1} \propto T, \quad (15)$$

$$R_H \propto \xi_{AF}^2 \propto \frac{1}{T}, \quad (16)$$

$$\cot \Theta_H \propto T^2. \quad (17)$$

These well reproduce the observed T -dependence of ρ_{xx} , R_H , and $\cot \Theta_H$ of CeRhIn₅ and CeCoIn₅ shown in Figs. 2 (a) and (b) and Figs 7 (a), (b), and (c). We note

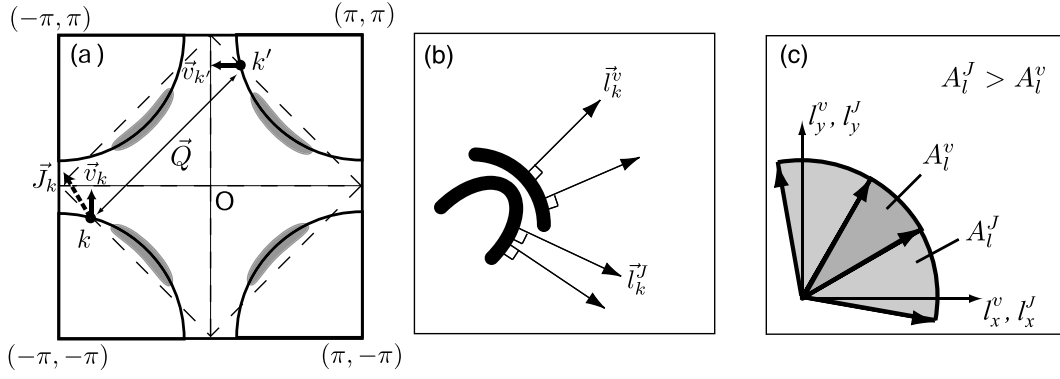


Fig. 14. (a) 2D Fermi surface. In the presence of strong AF fluctuations, \mathbf{v}_k is strongly coupled to $\mathbf{v}_{k'} = \mathbf{v}_k + \mathbf{Q}$ through a AF nesting vector \mathbf{Q} . Shaded area represents cold spots. Solid arrows indicate \mathbf{v}_k and $\mathbf{v}_{k'}$. Dashed arrow indicates \mathbf{J}_k . (b) Fermi surface with respect to \mathbf{v}_k and \mathbf{J}_k around a cold spot. The curvature of the Fermi surface can be strongly enhanced. (c) Swept area with respect to \mathbf{J}_k and that with respect to \mathbf{v}_k around a cold spot. A_l^J can be strongly enhanced from A_l^v .

that a recent calculation based on the band structure of CeCoIn₅ is quantitatively compatible with the enhancement of R_H below T_{coh} .⁶⁴

Enhancement of the amplitude of R_H at low temperatures has been reported for other quasi-2D strongly correlated systems, κ -(BEDT-TTF)₂Cu(NCS)₂⁶⁵⁻⁶⁷ and $R_{2-x}\text{Bi}_x\text{Ru}_2\text{O}_7$ ($R = \text{Sm}$ and Eu).⁶⁸ In addition, enhancement has also been reported for the 3D strongly correlated system V_{2-y}O_3 .⁶⁹ It has been shown that backflow plays an important role even in a 3D system, irrespective of the fact that the backflow vanishes in the $d = \infty$ limit. Therefore, the enhancement of the Hall coefficient in these three strongly correlated systems may relate to the backflow mechanism, though the T -dependence of the transport coefficients seem to be very different from those of CeMIn₅ and high- T_c cuprates.

We also note that in addition to these dc Hall effect, recent measurements of the high frequency ac Hall effect for high- T_c cuprates have reported anomalous T - and ω -dependence which exhibit a striking deviation from the Fermi liquid behavior.^{70,71} This behavior has been discussed in the light of the backflow effect.⁷²

4.3 Modified Kohler's rule

By definition, the magnetoresistance is given by

$$\frac{\Delta\rho_{xx}(H)}{\rho_{xx}(0)} = -\frac{\Delta\sigma_{xx}(H)}{\sigma_{xx}(0)} - \left(\frac{\sigma_{xy}(H)}{\sigma_{xx}(0)}\right)^2. \quad (18)$$

Using the relation $\Delta\sigma_{xx}(H)/\sigma_{xx}(H)^2 \sim \tau_{cold}^{-1}$, given by Eqs. (11) and (12), the magnetoresistance is obtained as

$$\frac{\Delta\rho_{xx}(H)}{\rho_{xx}(0)} = (\tan\Theta_H)^2 \cdot \left(\frac{\sigma_{xx}(H)}{\sigma_{xx}(0)}\right)^2 \cdot (C-1), \quad (19)$$

where C is a constant and is much larger than unity for CeMIn₅. Since $\sigma_{xx}(H)/\sigma_{xx}(0) \simeq 1$ at low fields, $\Delta\rho_{xx}(H)/\rho_{xx}(0)$ should be well scaled by $\tan^2\Theta_H$. Thus Eq. (6) holds for a theory in which the backflow effect is taken into account for the Fermi liquid ground state.

Since

$$\Delta\rho_{xx}(H)/\rho_{xx}(0) \sim \xi_{AF}^4 \tau_{cold}^2 H^2, \quad (20)$$

the P - and H -dependence of the magnetoresistance is governed by the P - and H -dependence of ξ_{AF} . As shown in Figs. 8 (a), (b), and (c), the magnetoresistance shows an anomalous concave downward curvature at $P < P^*$ (see Figs. 1 (a) and (b)), while such a behavior is not observed at $P > P^*$. Since the AF fluctuations are dramatically suppressed by magnetic fields at $P < P^*$,^{33,34,36,57} as discussed in §4.1, ξ_{AF} is rapidly reduced by magnetic fields. On the other hand, at $P > P^*$ where the AF fluctuation is already suppressed in zero field, ξ_{AF} is insensitive to the magnetic field. Thus the P - and H -dependence of the magnetoresistance in CeCoIn₅ and CeRhIn₅ reinforce the conclusion that AF fluctuations near the QCP play an essential role in determining the transport properties.

4.4 Impurity and pseudogap effects on the Hall effect

Having established the evidence for the importance of AF fluctuations on the electron transport properties, we next discuss the influence of impurities and the pseudogap on the Hall effect at low temperatures.

The amplitude of R_H is reduced at low temperatures in CeCoIn₅ and CeRhIn₅ at $P < P_c$, while such a reduction does not occur in CeRhIn₅ at $P > P_c$ (see Figs. 4 (a) and (b) and Fig. 5). We note that there are two possible origins for this: impurities and pseudogap formation.

We first discuss why region-(I) illustrated in Fig. 13 is present in CeCoIn₅ while it is absent in CeRhIn₅ at $P > P_c$. We note that this can be accounted for by considering the impurity scattering effect. The scattering time $\tau(\phi)$ can be taken to be the sum of an isotropic impurity part and anisotropic inelastic part:

$$\tau(\phi) = \frac{1}{\tau_{imp}^{-1} + \tau_{inel}(\phi)^{-1}}. \quad (21)$$

In region-(II) where inelastic scattering due to AF fluctuation dominates, backflow becomes important. However, as the temperature is lowered, isotropic impurity scattering becomes important ($\tau_{imp}^{-1} > \tau_{inel}^{-1}$). As a result, the influence of AF fluctuation on the Hall effect is reduced and the scattering become isotropic as shown

in Fig. 13 (b). In this situation, the backflow effect is greatly reduced¹⁸ and R_H is expected to approach the Fermi liquid value. The fact that R_H at $P = 2.51$ GPa in CeCoIn₅ approaches R_H of LaCoIn₅ seems to support this. (At $P = 0$ and 1.04 GPa, R_H does not recover to R_H^{La} in region-(I), because the system undergoes a superconducting transition.) To obtain more insight into the impurity effect, we compare the resistivity values at the temperatures T_m where the amplitude of R_H begin to decrease with decreasing T . The values of T_m at $P = 0, 1.04,$ and 2.51 GPa obtained from Fig. 4 (b) are ~ 4 K, 6 K, and 20 K, respectively. The values of ρ_{xx}^{mag} at T_m are $\sim 6.6, 4.9,$ and $6.1 \mu\Omega\text{cm}$ at $P=0, 1.04,$ and 2.51 GPa, respectively. Thus ρ_{xx}^{mag} at T_m have similar values, which are nearly P -independent. This can be seen by the hatched region in Fig. 2 (c).

Moreover, the impurity scenario naturally explains the absence of region-(I) in CeRhIn₅ at $P > P_c$. According to recent NMR T_1^{-1} measurements in the superconducting state, the impurity concentration in CeRhIn₅ is lower than that in CeCoIn₅, indicating that the impurity scattering in CeRhIn₅ is expected to be less important than in CeCoIn₅. Based on this finding, we conclude that *impurity scattering seriously influences the low temperature Hall effect*.

On the other hand, the origin of the reduction of the amplitude of R_H observed in the AF metallic regime of CeRhIn₅ seems to be more complicated. In fact, in contrast to CeCoIn₅, ρ_{xx} at different pressures have very different values at T_m , as shown by the dashed arrows in the inset of Fig. 5. We thus speculate that the reduction of ξ_{AF} due to the formation of a gap in the magnetic excitation is a primary cause of the reduction in the amplitude of R_H , because of the following reason.

Recent nuclear quadrupole resonance measurements indicate that the NMR T_1^{-1} exhibits a peak at T_{PG} above T_N ,⁷³ indicating a reduction of the AF correlation below T_{PG} . This behavior has been discussed in terms of gap formation in the spin excitation or a possible formation of a pseudogap in analogy to high- T_c cuprates. In Fig. 15, the pressure dependence of T_{PG} reported in Ref. [73] is plotted. As seen in Fig. 15, T_m is located close to T_{PG} . This implies a close relationship between the Hall effect and pseudogap formation. In this situation, the anisotropy of the inelastic scattering time due to AF spin fluctuations is expected to be seriously reduced by the suppression of magnetic scatterings, which gives rise to the situation illustrated in Fig. 13 (b). More detailed investigation is necessary to clarify this issue.

4.5 Hall effect and QCP

As discussed in §1, the evolution of the Fermi surface when crossing the QCP is an important issue in strongly correlated electron systems. Two contrary views have been proposed. Theories based on SDW predict a continuous change of the Fermi surface,^{53,54} while theories based on the breakdown of composite Fermions predict a jump of the Fermi surface volume at the QCP.⁴ As pointed out in Ref. [4], Hall measurements that can probe the Fermi surface are important for clarifying this

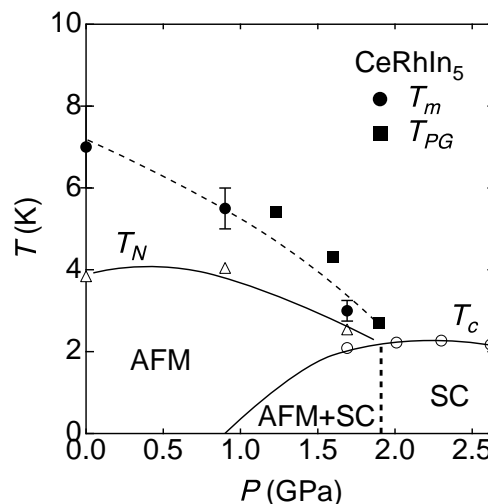


Fig. 15. Pressure dependence of the temperature at which the amplitude of R_H exhibits a maximum, T_m (filled circle), the pseudogap temperature determined by NMR relaxation rate T_{PG} (filled squares), and the Néel temperature T_N in the AF metallic regime of CeRhIn₅ ($P < P_c$).

controversial issue. According to the SDW picture, the Hall coefficient is expected to change continuously when crossing the QCP, while according to the picture of the breakdown of composite Fermions, the Hall coefficient is expected to jump at the QCP.⁴

As shown in Fig. 6, $|R_H^{\max}|$ for CeRhIn₅ at $\mu_0 H = 0$ increases rapidly as P_c is approached from either the AF metallic ($P < P_c$) or superconducting ($P > P_c$) regimes without exhibiting a jump at P_c . At $\mu_0 H = 7$ T, the enhancement of $|R_H^{\max}|$ is strongly reduced and exhibits a broad maximum at a pressure slightly higher than P_c . Recently it has been reported that the QCP slightly increases from P_c under a magnetic field and is located at ~ 2.1 GPa at $\mu_0 H = 7$ T.⁷⁴ Thus $|R_H^{\max}|$ in CeRhIn₅ appears to exhibit a maximum at or in the vicinity of the QCP without showing a jump. These results lead us to consider that a transition from AF metal with a small Fermi surface to a Fermi liquid with a large Fermi surface at the QCP suggested in Ref. [4] is unlikely to occur in CeRhIn₅. This Hall behavior in CeRhIn₅ is in striking contrast to the recent Hall measurements on YbRh₂Si₂, in which the Hall coefficient exhibits a discontinuous jump at the QCP.⁷⁵

4.6 Multiband effects

We here stress that the multiband effect is very unlikely to be an origin of the observed magnetotransport anomalies in CeMIn₅.

Real heavy fermion systems possess multiple Fermi surfaces with different sizes. According to dHvA experiments, quasiparticle masses on larger or smaller Fermi surfaces are, respectively, heavier or lighter in general. One may consider that lighter quasiparticles on smaller Fermi surfaces would be the main contribution to the transport phenomena, irrespective of the small area of the Fermi surface. However, it is well known that

the Kadowaki-Woods relation, $A\gamma^{-1} = 10^{-5}/\frac{1}{2}N(N-1)\mu\Omega\text{cm}(\text{mol}\cdot\text{K}/\text{mJ})^2$, holds for many heavy fermion superconductors, where A is the coefficient of the T^2 term in the resistivity, γ is the T -linear specific heat coefficient, and N is the f -orbital degeneracy.⁷⁶ This fact suggests that the transport phenomena are governed by larger Fermi surfaces with heavier masses in many compounds.

First of all, that Kohler's rule holds for LaRhIn₅ over four orders of magnitude of $\Delta\rho_{xx}/\rho_{xx}$ implies that the multiband effect is not important for the magnetotransport in CeMIn₅. Moreover, as we have discussed, the anomalous behaviors of ρ_{xx} , R_H , and $\Delta\rho_{xx}/\rho_{xx}$ in CeMIn₅ are satisfactorily scaled by a single parameter ξ_{AF} for a wide range of T , H , and P . This fact strongly suggests that the transport phenomena are caused by a single large Fermi surface composed of heavy quasiparticles. However, CeMIn₅ is a multiband system; the 13th and 14th bands give small and large hole-like Fermi surfaces, respectively, while the 15th and 16th bands give large and small electron-like Fermi surfaces, respectively.⁷⁷ One might consider that the small electron-like Fermi surfaces would be the origin of the huge negative R_H in CeMIn₅ near the AF QCP. However, this possibility is ruled out by the following argument.

We here discuss the possible multiband effect on the Hall coefficient by considering a two-band model (α, β). We express the Hall coefficient and the conductivity in each band as ($R_H^\alpha = 1/n^\alpha e$, σ_{xx}^α) or ($R_H^\beta = 1/n^\beta e$, σ_{xx}^β). Here we assume $R_H^\alpha > R_H^\beta > 0$. Then, the Hall coefficient of this system is

$$R_H = R_H^\alpha \frac{x^2 + R_H^\beta/R_H^\alpha}{(x+1)^2}, \quad (22)$$

where $x = \sigma_{xx}^\alpha/\sigma_{xx}^\beta$. We can show that $R_H^{\text{max}} = R_H^\alpha$ at $x = \infty$, and $R_H^{\text{min}} = R_H^\beta \frac{R_H^\beta/R_H^\alpha + 1}{(R_H^\beta/R_H^\alpha + 1)^2} \lesssim R_H^\beta$ at $x = R_H^\beta/R_H^\alpha$. It is easy to see that

$$R_H \sim R_H^\alpha \quad \text{for } \sigma_{xx}^\alpha \gtrsim \sigma_{xx}^\beta, \quad (23)$$

$$R_H \sim R_H^\beta \quad \text{for } \sigma_{xx}^\alpha \ll \sigma_{xx}^\beta. \quad (24)$$

Therefore, the assumption $R_H^\alpha/R_H^\beta = n^\beta/n^\alpha = 30-50$ is necessary to explain the experimental results of the Hall effect in CeMIn₅. According to the band calculation, $n(\text{15th band})/n(\text{16th band}) = 0.626/0.030 = 21$. In CeCoIn₅ at ambient pressure, Eq. (23) should be satisfied for $T \gtrsim T_c$, whereas Eq. (24) has to be realized for $T \sim T_{coh}$. That is, the most conductive band changes from α to β with increasing temperature. At $P = 2.51$ GPa, on the other hand, Eq. (24) should be satisfied below T_{coh} . In this case, the most conductive band is always β . However, we see in Fig. 2 (c) that ρ_{xx}^{mag} at $P = 0$ and 2.51 GPa shows very similar T/T_{coh} -dependences. This experimental result apparently contradicts the above mentioned scenario. Moreover, the present two-band model cannot explain the enhancement of the magnetoresistance and the Nernst coefficient below T_{coh} , because both are independent of the band filling in the Bloch-Boltzmann approximation.

4.7 Thermoelectric effects

In addition to the non-Fermi liquid behavior of the electron transport properties, the thermoelectric effects, such as Nernst coefficient and thermoelectric power, have been reported to be anomalous in high- T_c cuprates. Especially, a giant enhancement of the Nernst coefficient ν_H three orders of magnitude larger than that expected in conventional metals has been reported in the normal state of high- T_c cuprates in the underdoped and optimally doped regimes.¹⁵ Recently, it has been reported that the amplitude of ν_H in the normal state of CeCoIn₅ at ambient pressure is also strikingly enhanced by more than three orders of magnitude, compared with conventional metals.³⁷ The sign of ν_H is positive in cuprates while it is negative in CeCoIn₅.

The origin of the giant Nernst signal is controversial. On the one hand, the origin has been discussed in the light of vortex-like excitations in high- T_c cuprates. On the other hand, it has been suggested that the origin can be explained in a unified way in the framework of the backflow effect.⁷⁸ Whether the giant Nernst coefficients in high- T_c cuprates and CeCoIn₅ have the same origin should be scrutinized. In CeCoIn₅, the giant Nernst effect gradually fades with the application of a magnetic field. This phenomenon, like the anomalously large Hall coefficient, may reflect a large energy-dependence of the scattering time and highly anisotropic backflow due to the presence of AF fluctuations. A study of the pressure dependence of the Nernst effect in CeMIn₅ is necessary to clarify this issue.

5. Conclusions

In summary, we have performed a systematic study of the magnetotransport properties of quasi 2D heavy fermion CeMIn₅ (M :Rh and Co) under pressure, ranging from the AF metal state to the Fermi liquid state through the non-Fermi liquid state.

In CeMIn₅, the amplitude of the Hall coefficient is dramatically enhanced with decreasing temperature and attains a value much larger than $|1/ne|$ at low temperatures. Furthermore, the magnetoresistance exhibits striking violation of Kohler's rule. These findings are in sharp contrast to the behavior of LaMIn₅ with a similar electronic structure. We found that the dc-resistivity is proportional to T , the cotangent of the Hall angle $\cot \Theta_H$ varies as T^2 , and the magnetoresistance is well scaled by the tangent of the Hall angle as $\Delta\rho_{xx}/\rho_{xx} \propto \tan^2 \Theta_H$. These non-Fermi liquid behavior observed in the electron transport are remarkably pronounced with approaching the AF QCP. The T -, H -, and P -dependence of the dc-resistivity, Hall coefficient and magnetoresistance definitely indicate that AF fluctuations play a crucial role in determining the non-Fermi liquid behavior of the electron transport phenomena.

We have shown that the anomalous electron transport properties can be accounted for in terms of a recent theory in which hot and cold spots around the Fermi surface and the backflow effect are taken into account; all of the anomalous behavior of dc-resistivity, Hall effect, and magnetoresistance are well scaled by a single parameter,

the AF correlation length $\xi_{AF} \propto 1/\sqrt{T+\theta}$, for a wide range of the parameters, T , H , and P .

Several anomalous transport properties observed in $CeMIn_5$ bear a striking resemblance to the normal-state properties of high- T_c cuprates, indicating universal transport properties of strongly correlated quasi 2D electron systems in the presence of strong AF fluctuations. Thus the present results may also prove relevant for the debate on the anomalous normal-state properties of high- T_c cuprates, holding the promise of bridging our understanding of heavy fermion systems and cuprates.

Acknowledgment

We thank M. Sato and K. Yamada for stimulating discussions. This work was partly supported by a Grant-in-Aid for Scientific Research from the Ministry of Education, Culture, Sports, Science and Technology. One of the authors (Y. N.) was supported by the Research Fellowships of the Japan Society for the Promotion of Science for Young Scientists.

- 1) C. M. Hurd: *The Hall Effect in Metal and Alloys* (Plenum, New York, 1972).
- 2) A. B. Pippard: *Magnetoresistance in Metals* (Cambridge University Press, 1989).
- 3) T. Moriya, and T. Takimoto: J. Phys. Soc. Jpn, **64** (1995) 960.
- 4) P. Coleman, C. Pépin, Q. Si and R. Ramazashvili: J.Phys.: Condens. Matter **13** (2001) R723.
- 5) S. Sachdev: *Quantum Phase Transitions*, (Cambridge University Press, Cambridge UK 1999).
- 6) M. Sigrist and K. Ueda: Rev. Mod. Phys. **63** (1991) 239.
- 7) P. Thalmeier, and G. Zwicknagl: *Handbook on the Physics and Chemistry of Rare Earths* (Elsevier, Amsterdam,2005) Vol.34, 135.
- 8) V.P. Mineev and K.V.Samokhin: *Introduction to Unconventional Superconductivity* (Gordon and Breach Science Publishers, 1999).
- 9) see, e.g., N. P. Ong: *Physical Properties of High Temperature Superconductors*, edited by D.M. Ginsberg (World Scientific, Singapore, 1992), Vol.2.
- 10) J. Takeda, N. Nishikawa, and M. Sato: Physica C **231** (1994) 293.
- 11) Y. Ando, Y. Kurita, S. Komiya, S. Ono, and K. Segawa: Phys. Rev. Lett. **92** (2004) 197001.
- 12) T.R. Chien, Z.Z. Wang, and N.P. Ong, Phys. Rev. Lett: **67** (1991) 2088.
- 13) P.W. Anderson: Phys. Rev. Lett. **67** (1991) 2092.
- 14) J.M. Harris, Y.F. Yan, P. Matl, N.P. Ong, P.W. Anderson, T. Kimra and K. Kitazawa: Phys. Rev. Lett. **75** (1995) 1391.
- 15) Z.A. Xu, N.P. Ong, Y. Wang, T. Kakeshita, and S. Uchida: Nature 406 (2000) 486.
- 16) B.P. Stojković and D. Pines: Phys. Rev. B **55** (1997) 8576.
- 17) L.B. Ioffe and A.J. Millis: Phys. Rev. B **58** (1998) 11631.
- 18) H. Kontani, K. Kanki, and K. Ueda: Phys. Rev. B **59** (1999) 14723, and K. Kanki and H. Kontani: J. Phys. Soc. Jpn, **68** (1999) 1614.
- 19) A. Rosch: Phys. Rev. B **62** (2000) 4945.
- 20) N.E. Hussey: Eur. Phys. J. B **31** (2003) 495, and references therein.
- 21) N.P. Ong and P.W. Anderson: Phys. Rev. Lett. **78** (1997) 977.
- 22) C. Petrovic, P.G. Pagliuso, M.F. Hundley, R. Movshovich, J.L. Sarrao, J.D. Thompson, Z. Fisk and P. Monthoux: J. Phys. Condens. Matter **13** (2001) L337.
- 23) H. Hegger, C. Petrovic, E.G. Moshopoulou, M.F. Hundley, J.L. Sarrao, Z. Fisk, and J.D. Thompson: Phys. Rev. Lett. **84** (2000) 4986.
- 24) C. Petrovic, R. Movshovich, M. Jaime, P.G. Pagliuso, M.F. Hundley, J.L. Sarrao, Z. Fisk, and J.D. Thompson: Europhys. Lett. **53** (2001) 354.
- 25) R. Settai, H. Shishido, S. Ikeda, Y. Murakawa, M. Nakashima, D. Aoki, Y. Haga, H. Harima and Y. Onuki: J. Phys.: Condens. Matter **13** (2001) L627.
- 26) H. Shishido, R. Settai, D. Aoki, S. Ikeda, H. Nakawaki, N. Nakamura, T. Iizuka, Y. Inada, K. Sugiyama, T. Takeuchi, K. Kindo, T.C. Kobayashi, Y. Haga, H. Harima, Y. Aoki, T. Namiki, H. Sato and Y. Onuki: J. Phys. Soc. Jpn **71** (2002) 162.
- 27) G.-q. Zeng, K. Tanabe, T. Mito, S. Kawasaki, Y. Kitaoka, D. Aoki, Y. Haga and Y. Onuki: Phys. Rev. Lett. **86** (2001) 4664.
- 28) Y. Kawasaki, S. Kawasaki, M. Yashima, T. Mito, G.-q. Zheng, Y. Kitaoka, H. Shishido, R. Settai, Y. Haga and Y. Onuki: J. Phys. Soc. Jpn. **72** (2003) 2308.
- 29) V. A. Sidorov, M. Nicklas, P.G. Pagliuso, J.L. Sarrao, Y. Bang, A.V. Balatsky and J.D. Thompson: Phys. Rev. Lett. **89** (2002) 157004.
- 30) G. Knebel, M-A. Méasson, B. Salce, D. Aoki, D. Braithwaite, J.P. Brison and J. Flouquet: J. Phys.: Condens. Matter **16** (2004) 8905.
- 31) R. A. Fisher, F. Bouquet, N.E. Phillips, M.F. Hundley, P.G. Pagliuso, J.L. Sarrao, Z. Fisk, and J.D. Thompson: Phys. Rev. B **65** (2002) 224509.
- 32) S. Ikeda, H. Shishido, M. Nakashima, R. Settai, D. Aoki, Y. Haga, H. Harima, Y. Aoki, T. Namiki, H. Sato and Y. Onuki: J. Phys. Soc. Jpn. **70** (2001) 2248.
- 33) A. Bianchi, R. Movshovich, I. Vekhter, P.G. Pagliuso and J.L. Sarrao: Phys. Rev. Lett. **91** (2003) 257001.
- 34) T. Tayama, A. Harita, T. Sakakibara, Y. Haga, H. Shishido, R. Settai and Y. Onuki: Phys. Rev. B **65** (2002) 180504.
- 35) Y. Kohori, Y. Yamato, Y. Iwamoto, T. Kohara, E.D. Bauer, M.B. Maple and J.L. Sarro: Phys. Rev. B **64**, (2001) 134526.
- 36) M. Yashima, S. Kawasaki, Y. Kawasaki, G.-q. Zheng, Y. Kitaoka, H. Shishido, R. Settai, Y. Haga and Y. Onuki: J. Phys. Soc. Jpn. **73** (2004) 2073.
- 37) R. Bel, K. Behnia, Y. Nakajima, K. Izawa, Y. Matsuda, H. Shishido, R. Settai and Y. Onuki: Phys. Rev. Lett. **92** (2004) 217002.
- 38) R. Movshovich, M. Jaime, J.D. Thompson, C. Petrovic, Z. Fisk, P.G. Pagliuso and J.L. Sarrao: Phys. Rev. Lett. **86** (2001) 5152.
- 39) H. Aoki, T. Sakakibara, H. Shishido, R. Settai, Y. Onuki, P. Miranovic and K. Machida: J Phys.: Condens Matter **16** (2004) L13.
- 40) K. Izawa, H. Yamaguchi, Y. Matsuda, H. Shishido, R. Settai and Y. Onuki: Phys. Rev. Lett. **87** (2001) 057002.
- 41) R.J. Ormeno, A. Sibley, C.E. Gough, S. Sebastian and I.R. Fisher: Phys. Rev. Lett. **88** (2002) 47005.
- 42) E.E.M. Chia, D.J. Van Harlingen, M. B. Salamon, B.D. Yanoff, I. Bonalde, and J.L. Sarrao: Phys. Rev. B **67** (2003) 014527.
- 43) P.M.C. Rourke, M.A. Tanatar, C.S. Turel, J. Berdeklis, C. Petrovic, and J.Y.T. Wei: Phys. Rev. Lett. **94** (2005) 107005 (2005).
- 44) W.K. Park, L. H. Greene, J. L. Sarrao, and J.D. Thompson: cond-mat/0606535
- 45) A. Vorontsov and I. Vekhter: Phys. Rv. Lett. **96** (2006) 237001.
- 46) H.A. Radovan, N.A. Fortune, T.P. Murphy, S.T. Hannahs, E.C. Palm, S.W. Tozer and D. Hall: Nature **425** (2003) 51, A. Bianchi, R. Movshovich, C. Capan, P.G. Pagliuso, J.L. Sarrao: Phys. Rev. Lett. **91** (2003) 187004, T. Watanabe, Y. Kasahara, K. Izawa, T. Sakakibara, Y. Matsuda, C.J. van der Beek, T. Hanaguri, H. Shishido, R. Settai and Y. Onuki: Phys. Rev. B **70** (2004) 020506, K. Kakuyanagi, M. Saitoh, K. Kumagai, S. Takashima, M. Nohara, H. Takagi and Y. Matsuda: Phys. Rev. Lett. **94** (2005) 047602.
- 47) Y. Kasahara, Y. Nakajima, K. Izawa, Y. Matsuda, K. Behnia, H. Shishido, R. Settai, and Y. Onuki: Phys. Rev. B **72** (2005)

- 214515.
- 48) A. Fert, and P.M. Levy: Phys. Rev. B **36** (1987) 1907.
- 49) P. Coleman, P.W. Anderson, and T.V. Ramakrishnan: Phys. Rev. Lett. **55** (1985) 414.
- 50) H. Kontani and K. Yamada: J. Phys. Soc. Jpn. **63** (1994) 2627.
- 51) Y. Nakajima, K. Izawa, Y. Matsuda, S. Uji, T. Terashima, H. Shishido, R. Settai, Y. Onuki, and H. Kontani: J. Phys. Soc. Jpn **73** (2004) 5.
- 52) Y. Nakajima, K. Izawa, Y. Matsuda, K. Behnia, H. Kontani, M. Hedo, Y. Uwatoko, T. Matsumoto, H. Shishido, R. Settai, and Y. Onuki: J.Phys. Soc. Jpn **75** (2006) 023705.
- 53) J.A. Hertz: Phys. Rev. B **14** (1976) 1165.
- 54) A.J. Millis: Phys. Rev. B **48** (1993) 7183.
- 55) M.F. Hundley, A. Malinowski, P.G. Pagliuso, J.L. Sarrao and J.D. Thompson: Phys. Rev. B. **70** (2004) 035113.
- 56) J. M. Ziman: *Electrons and Phonons* (1960).
- 57) J. Paglione, M. A. Tanatar, D. G. Hawthorn, E. Boaknin, R. W. Hill, F. Ronning, M. Sutherland, L. Taillefer, C. Petrovic, P. C. Canfield: Phys. Rev. Lett. **91** (2003) 246405.
- 58) T. Ebihara, N. Harrison, M. Jaime, S. Uji and J.C. Lashley: Phys. Rev. Lett. **93** (2004) 246401.
- 59) H. Kontani and K. Yamada: J. Phys. Soc. Jpn. **74** (2005) 155.
- 60) K. Yamada: *Electron Correlation in Metals* (Cambridge Univ. Press, 2004).
- 61) According to the self consistent renormalization theory, $\xi_{AF}^2 \propto T^{-3/2}$ just on the AF QCP in 3D systems. However, ξ_{AF}^2 exhibits a Curie-Weiss behavior for a wide range of temperature near the AF QCP.
- 62) N.P. Ong: Phys. Rev. B **43** (1991) 193.
- 63) H. Kontani: J. Phys. Soc. Jpn. **70** (2001) 1873.
- 64) S. Onari, H. Kontani and Y. Tanaka: Phys. Rev. B **73** (2006).
- 65) K. Katayama, T. Nagai, H. Taniguchi, K. Satoh, N. Tajima and R. Kato, to be published in J. Low Temp. Phys. (2006).
- 66) Y.V. Sushko, N. Shirakawa, K. Murata, Y. Kubo, N.D. Kushch, and E.B. Yagubskii: Synth. Met. **85** (1997) 1541.
- 67) H. Kontani and H. Kino: Phys. Rev. B **63** (2001) 134524.
- 68) S. Yoshii, K. Murata and M. Sato: FJ. phys. Soc. Jpn. **69** (2000) 17.
- 69) T.F. Rosenbaum, A. Husmann, S.A. Carter and J.M Honig: Phys. Rev. B **57** (1998) R13997.
- 70) J. Cerne, M. Grayson, D.C. Schmadel, G.S. Jenkins, H.D. Drew, R. Hughes, A. Dabkowski, J.S. Preston, and P.-J. Kung: Phys. Rev. Lett. **84** (2000) 3418.
- 71) M. Grayson, L.B. Rigal, D.C. Schmadel, H.D. Drew, and P.-J. Kung: Phys. Rev. Lett. **89** (2002) 037003.
- 72) H. Kontani: J. Phys. Soc. Jpn. **75** (2006) 013703.
- 73) S. Kawasaki, M. Yashima, T. Mito, Y. Kawasaki, G.-q. Zheng, Y. Kitaoka, D. Aoki, Y. Haga and Y. Onuki: J. Phys.: Condens. Matter **17** (2005) S889.
- 74) T. Park, F. Ronning, H.Q. Yuan, M.B. Salamon, R. Movshovich, J.L. Sarrao, and J.D. Thompson, *et al.*: Nature, 440 (2006) 65.
- 75) S. Paschen, T. Luhmann, S. Wirth, P. Gegenwart, O. Trovarelli, C. Geibel, F. Steglich, P. Coleman, Q. Si: Nature **432** (2004) 881.
- 76) N. Tsujii, H. Kontani and K. Yoshimura: Phys. Rev. Lett. **94** (2005) 057201.
- 77) T. Maehira, T. Hotta, K. Ueda and A. Hasegawa: J. Phys. Soc. Jpn. **72** (2003) 854.
- 78) H. Kontani: Phys. Rev. Lett. **89** (2003) 237003.